

QCD flux tubes across deconfinement phase transition

Leonardo Cosmai
INFN Bari



in collaboration with: **Paolo Cea, Francesca Cuteri, Alessandro Papa**



Lattice 2017
18-24 June 2017, Granada

Outline

- Introduction
- Flux Tubes in $SU(3)$ across deconfinement
- Conclusions

Acknowledgements

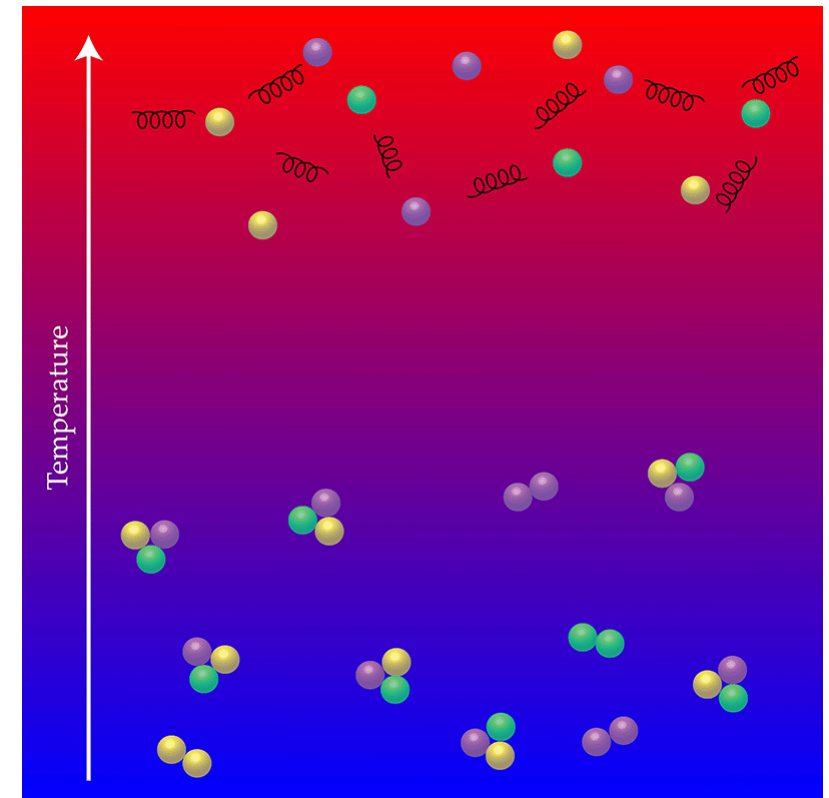
- Simulations have been performed at **CINECA** (on IBM NeXtScale "GALILEO", Lenovo NeXtScale "MARCONI", under **CINECA-INFN agreement**).



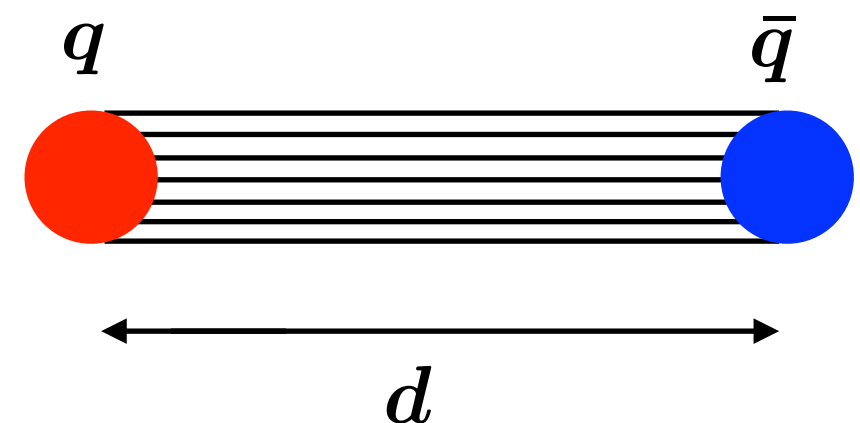
- This work was in part based on the **MILC** collaboration's public lattice gauge theory code. See <http://physics.utah.edu/~detar/milc.html>

Introduction

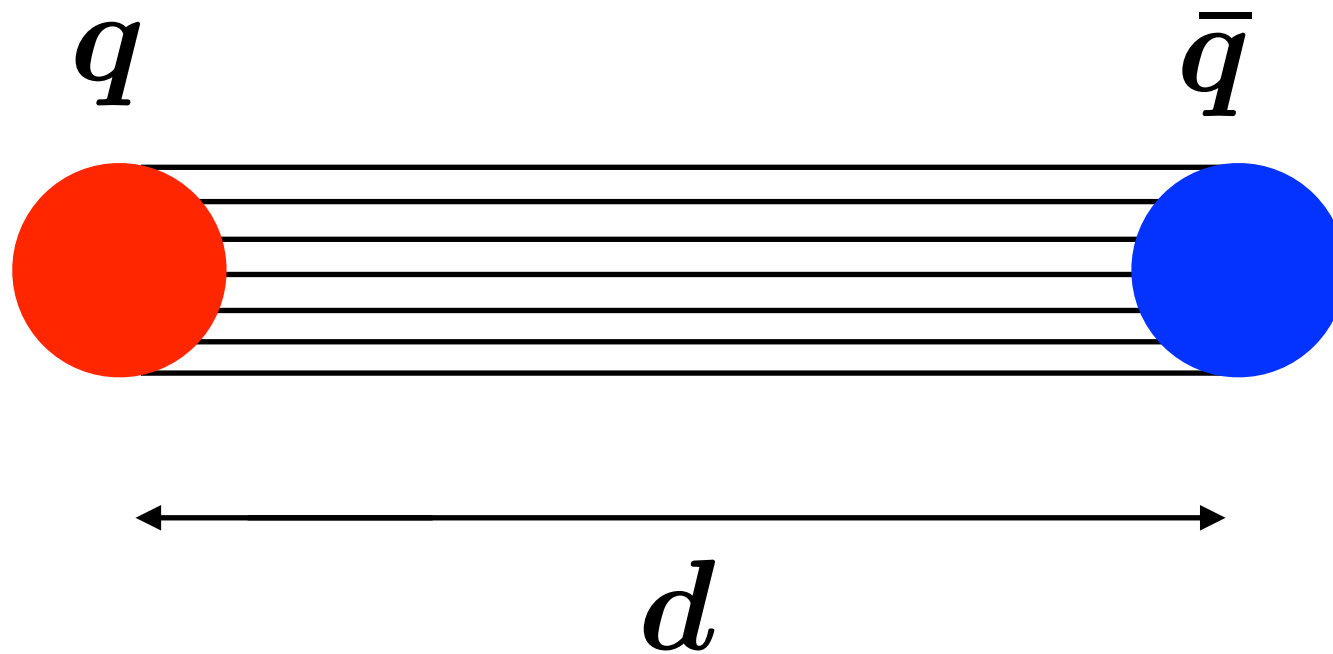
- Reaching a detailed understanding of color confinement is one of the central goals of nonperturbative studies of QCD.
- It is known since long that, in lattice numerical simulations, tubelike structures emerge by analyzing the chromoelectric fields between static quarks. Such tubelike structures naturally lead to a linear potential between static color charges and, consequently, to a direct numerical evidence of color confinement.



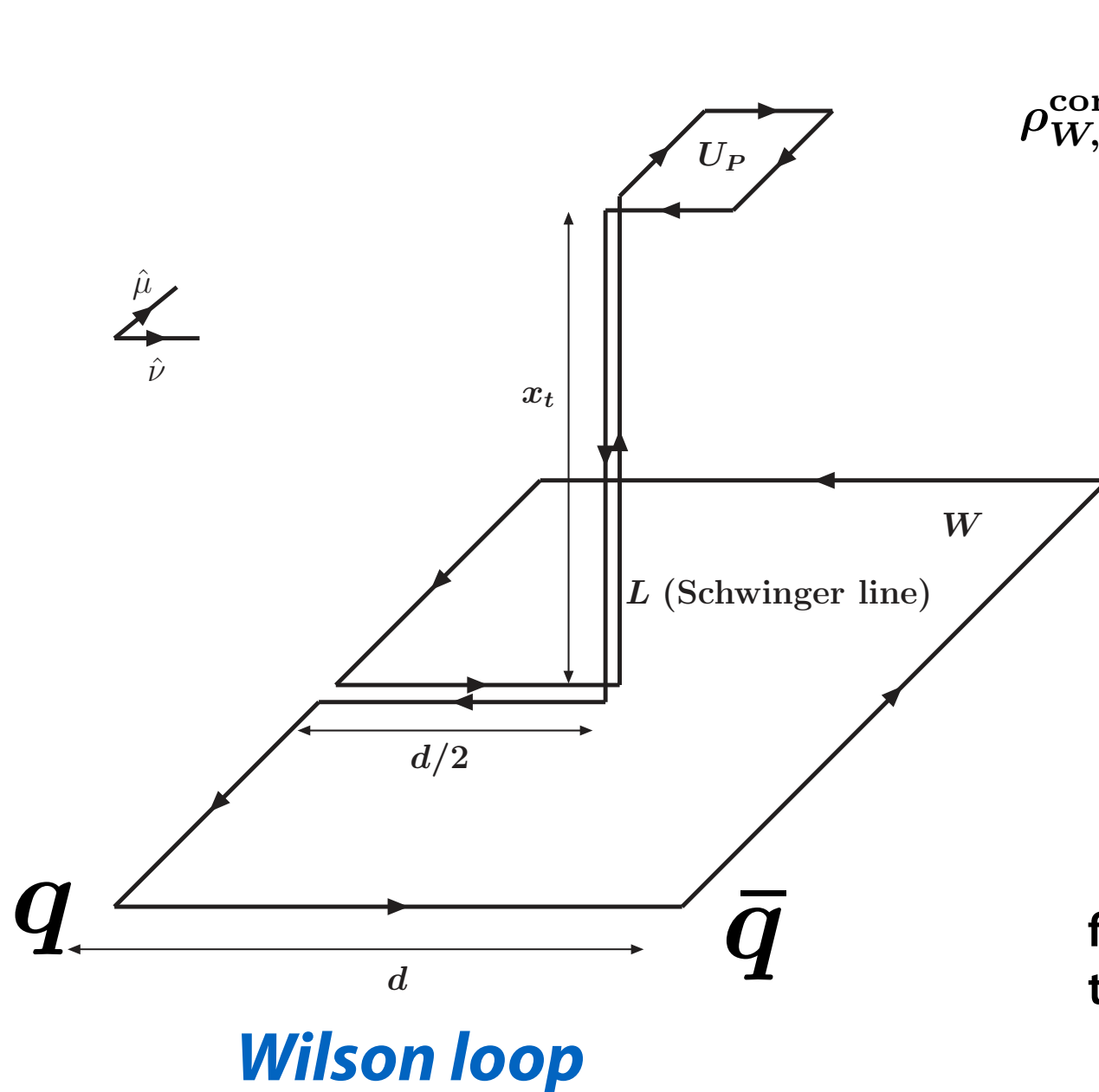
[Credit: APS/Joan Tycko]



*How to measure the chromoelectric field
on the lattice?*



To explore on the lattice the field configurations produced by a static quark-antiquark pair \rightarrow connected correlation function (*)



$$T = 0$$

$$\rho_{W,\mu\nu}^{\text{conn}} = \frac{\langle \text{tr} (W L U_P L^\dagger) \rangle}{\langle \text{tr}(W) \rangle} - \frac{1}{N} \frac{\langle \text{tr}(U_P) \text{tr}(W) \rangle}{\langle \text{tr}(W) \rangle}$$

$U_P = U_{\mu\nu}(x)$ plaquette in the (μ, ν) plane

L Schwinger line

N number of colors

$$\rho_W^{\text{conn}} \xrightarrow{a \rightarrow 0} a^2 g \left(\langle F_{\mu\nu} \rangle_{q\bar{q}} - \langle F_{\mu\nu} \rangle_0 \right)$$

$\langle \rangle_{q\bar{q}}$ average in the presence of a static quark-antiquark pair

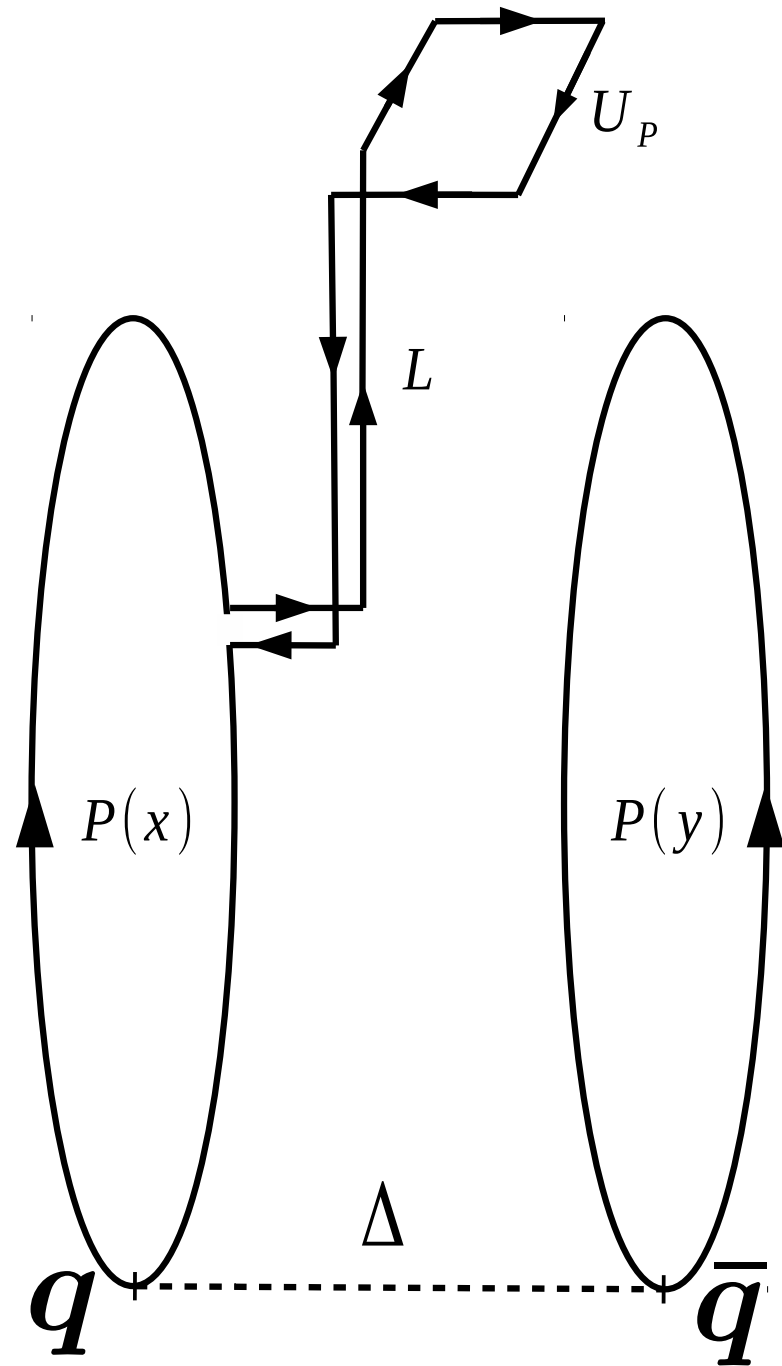
$\langle \rangle_0$ vacuum average (expected to vanish)

field strength tensor

$$F_{\mu\nu}(x) = \frac{1}{a^2 g} \rho_{W,\mu\nu}^{\text{conn}}(x)$$

(*) Di Giacomo, Maggiore, Oleinik, NPB347(1990)441
 Skala, Faber, Zach, NPB494(1997)293
 Kuzmenko, Simonov, PLB494(2000)81
 Di Giacomo, Dosch, Shevchenko, Simonov, Phys.Rept.372(2002)319

Polyakov loop correlator at $T \neq 0$



Polyakov loop

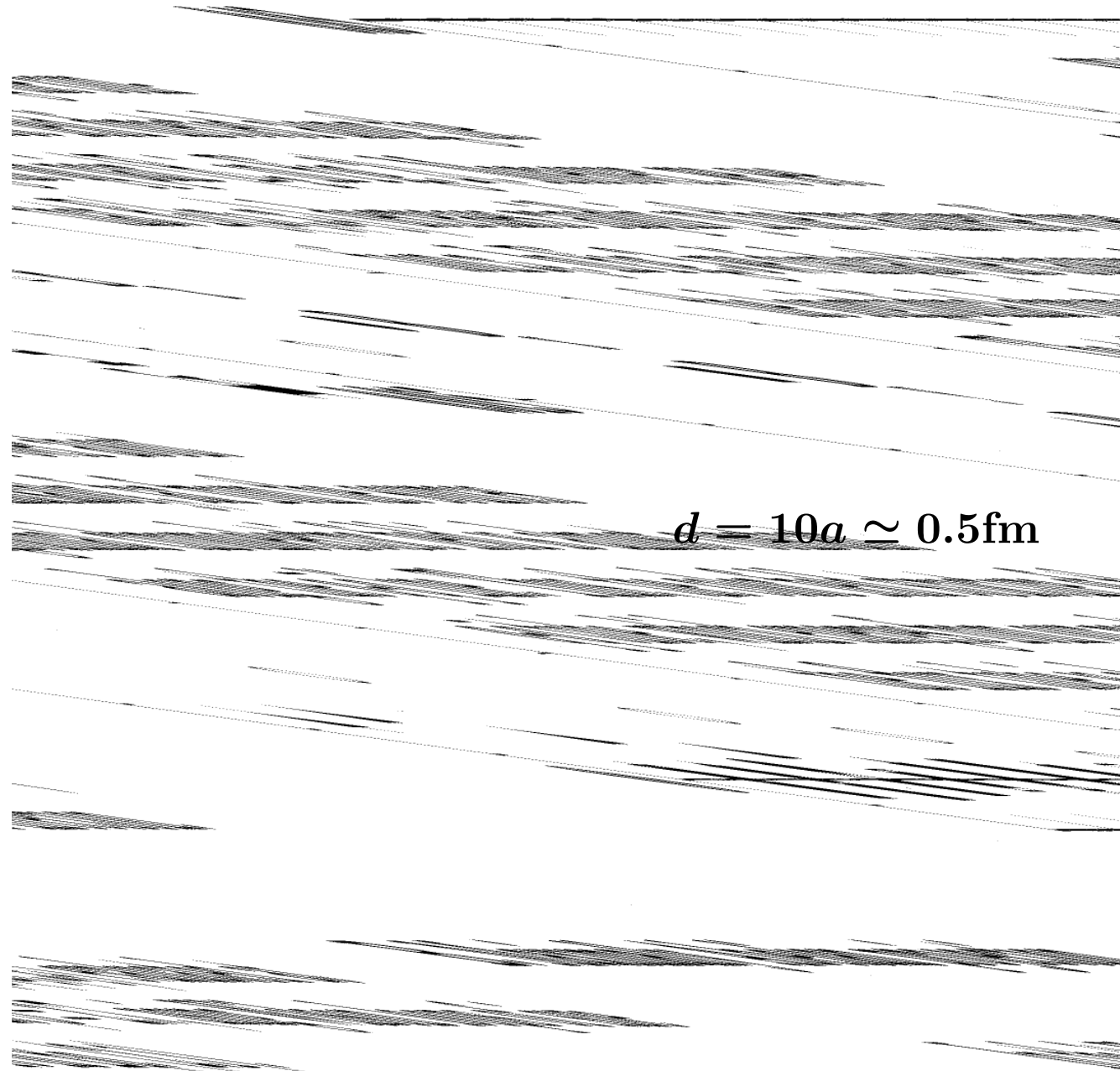
$T \neq 0$

$$\rho_{P,\mu\nu}^{\text{conn}} = \frac{\langle \text{tr}(P(x) L U_P L^\dagger) \text{tr} P^\dagger(y) \rangle}{\langle \text{tr}(P(x)) \text{tr}(P^\dagger(y)) \rangle} - \frac{1}{N} \frac{\langle \text{tr}(P(x)) \text{tr}(P^\dagger(y)) \text{tr}(U_P) \rangle}{\langle \text{tr}(P(x)) \text{tr}(P^\dagger(y)) \rangle}$$

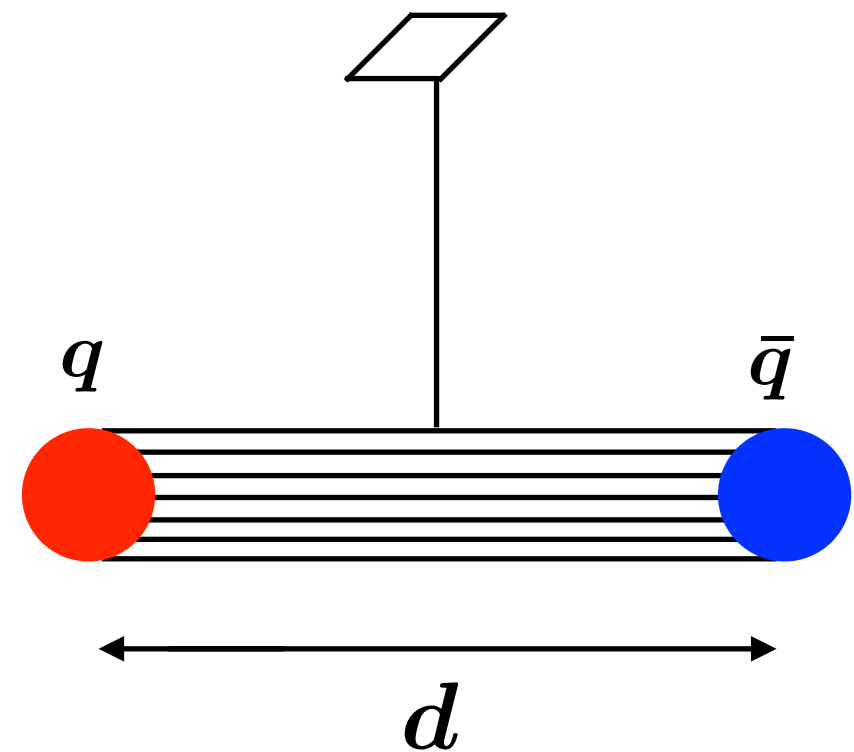
$$F_{\mu\nu}(x) = \frac{1}{a^2 g} \rho_{P,\mu\nu}^{\text{conn}}(x)$$

Chromoelectric longitudinal field

P. Cea and L.C., Phys. Rev.D52 (1995) 5152

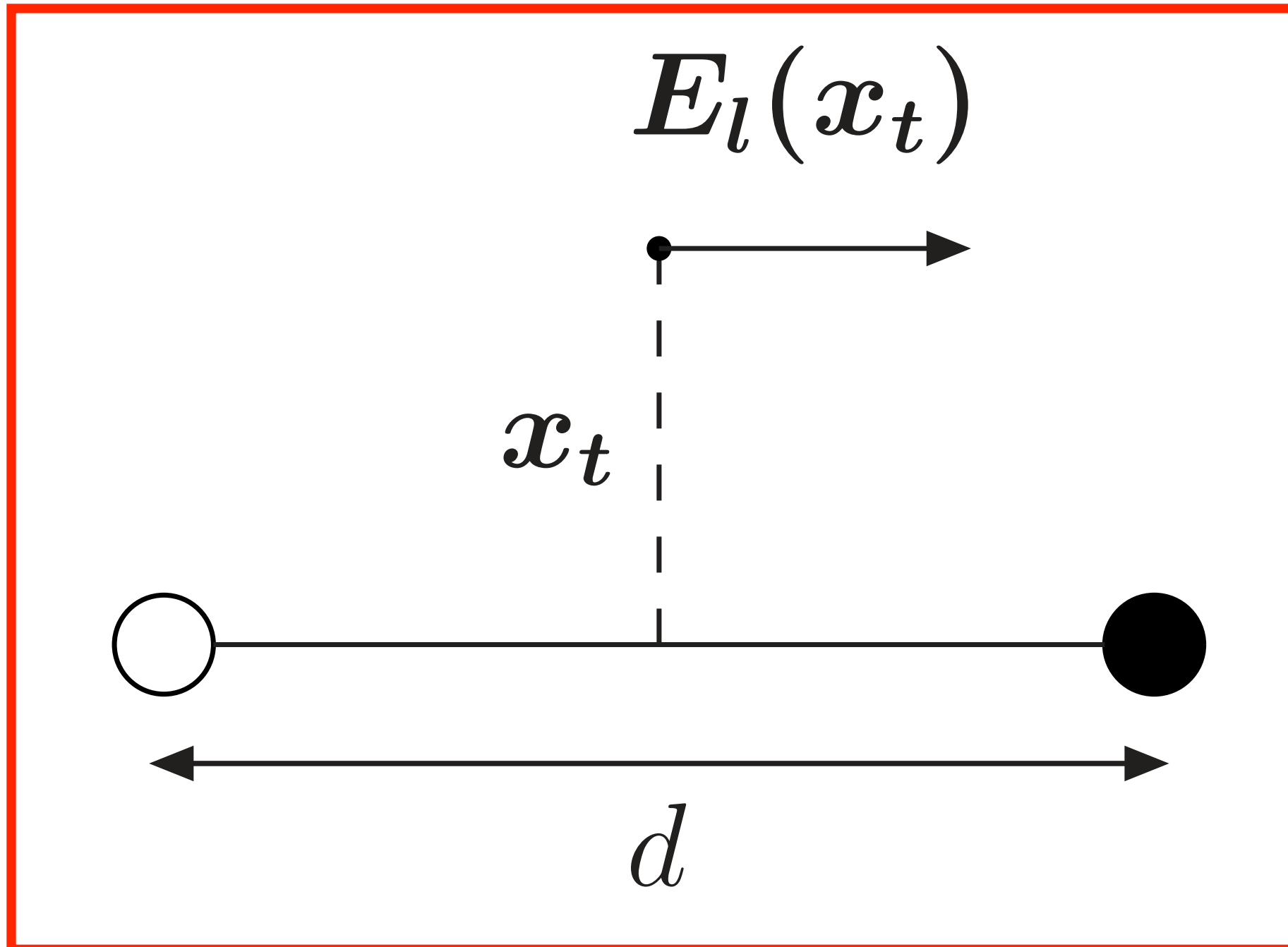


$$F_{\mu\nu}(x) = \frac{1}{a^2 g} \rho_{W,\mu\nu}^{\text{conn}}(x)$$



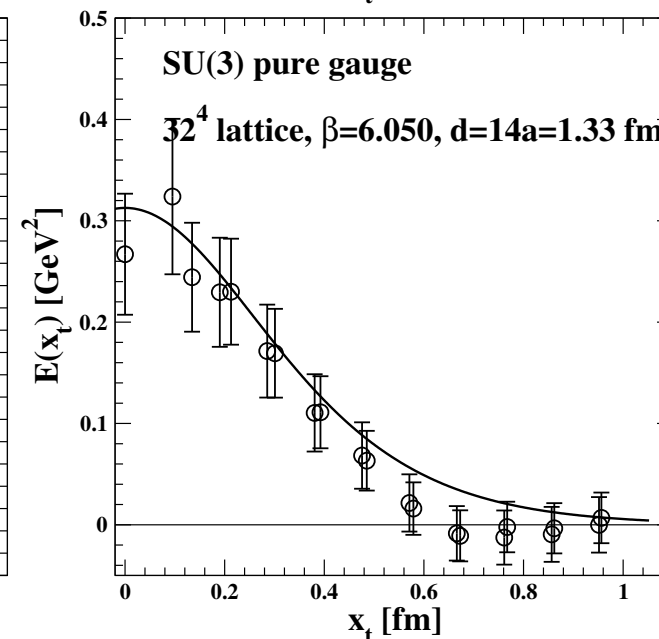
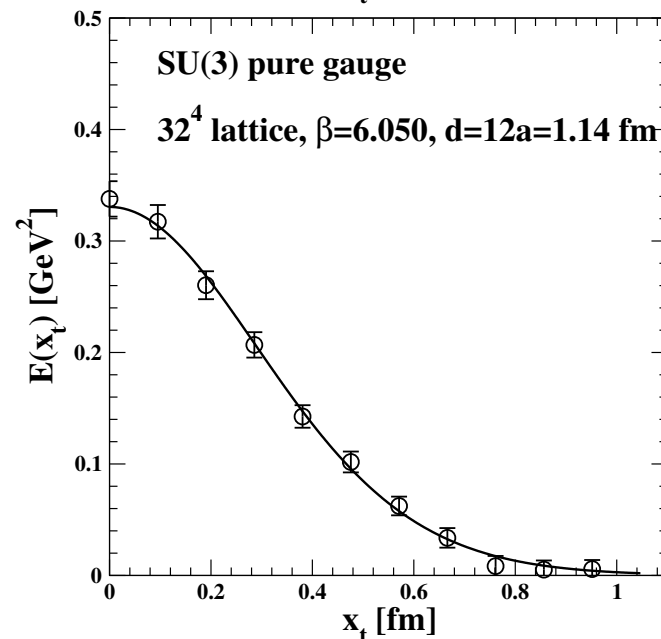
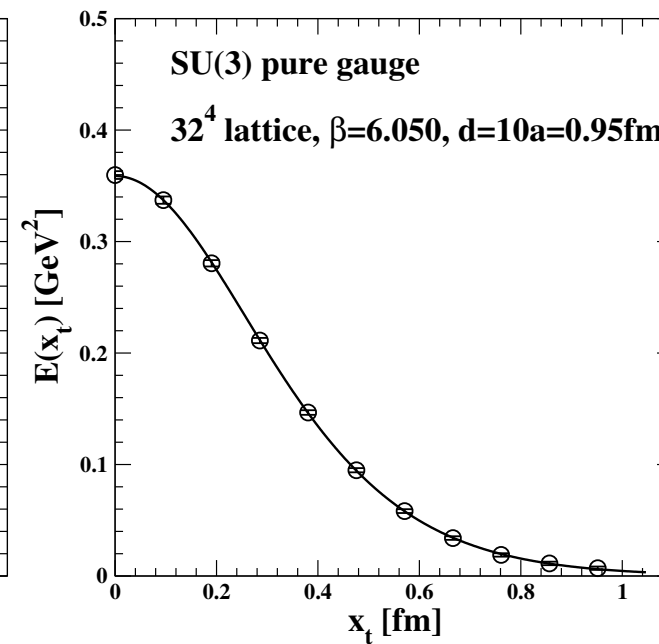
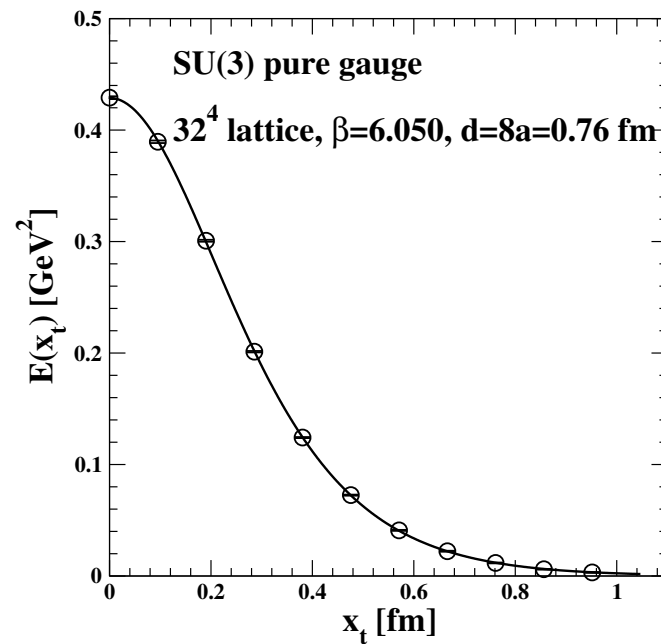
The flux tube is almost completely formed by the longitudinal chromoelectric field, which is constant along the flux tube (not too close to the sources) and decreases rapidly in the transverse direction.

The longitudinal chromoelectric field



SU(3) pure gauge $T=0$

(P.Cea, L.C., F. Cuteri, A.Papa, arXiv:1702.06437)



● falloff of the chromoelectric field along the transverse direction

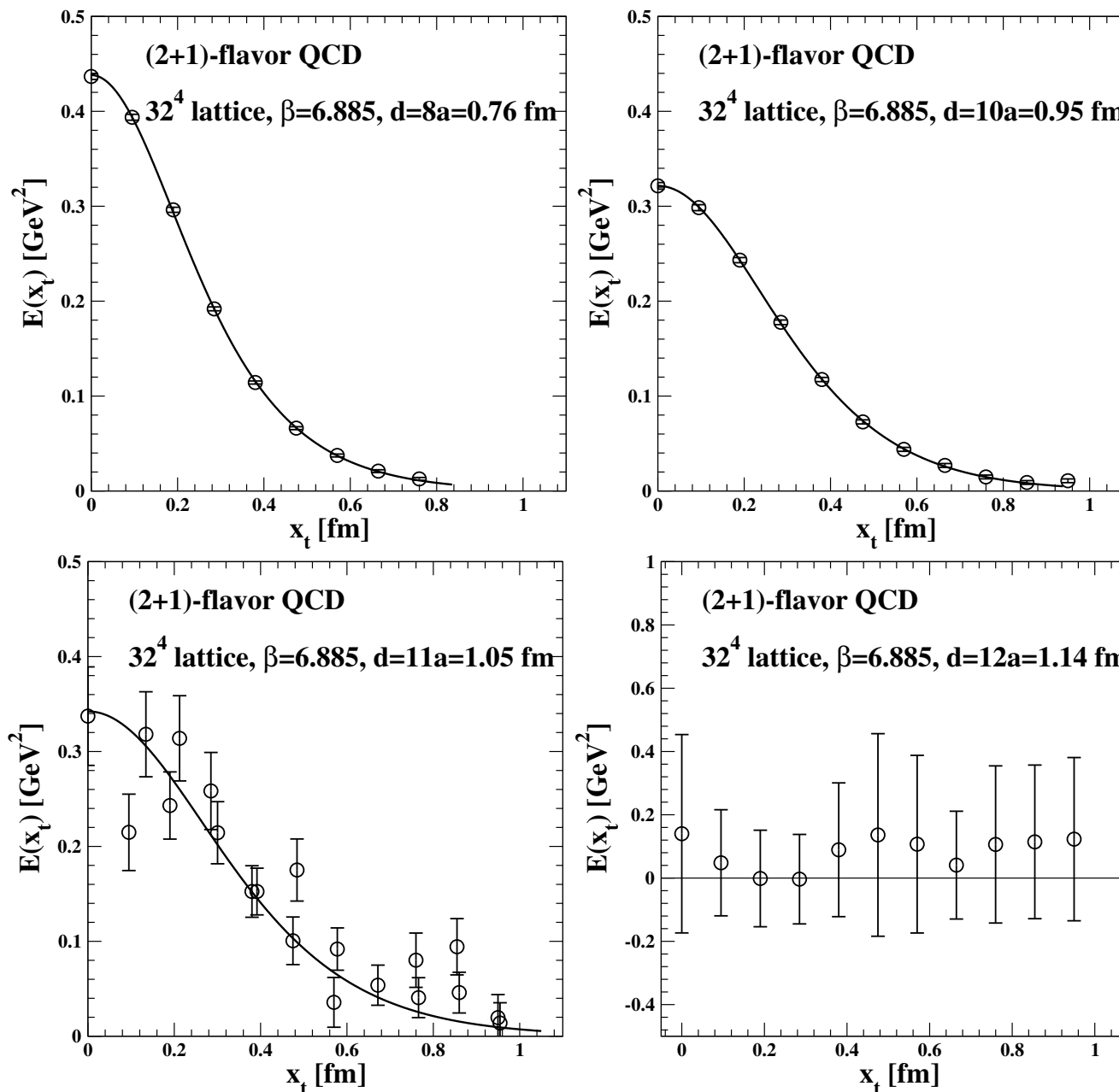
● almost constant transverse size of the flux tube independent of the distance between the sources

(2+1) flavors (HISQ fermions)



- falloff of the chromoelectric field along the transverse direction

- almost constant transverse size of the flux tube independent of the distance between the sources (comparable with pure gauge)



string breaking at $d \approx 1.14$ fm ?

(agreement with Bali et al., arXiv:hep-lat/0505012; Koch et al., arXiv:1511.04029)

FLUX TUBES IN $SU(3)$ ACROSS DECONFINEMENT

LATTICE SETUP

- lattice sizes: $40^3 \times 10, 48^3 \times 12$
- smoothing of the gauge configurations: several APE smearings for spatial links, one HYP smearing for temporal links
- scale setting: (Edwards, Heller, Klassen, Nucl. Phys. B517 (1998) 377)

$$(a \sqrt{\sigma})(g) = \frac{f_{\text{SU}(3)}(g^2) \{1 + 0.2731 \hat{a}^2(g) - 0.01545 \hat{a}^4(g) + 0.01975 \hat{a}^6(g)\}}{0.01364}$$

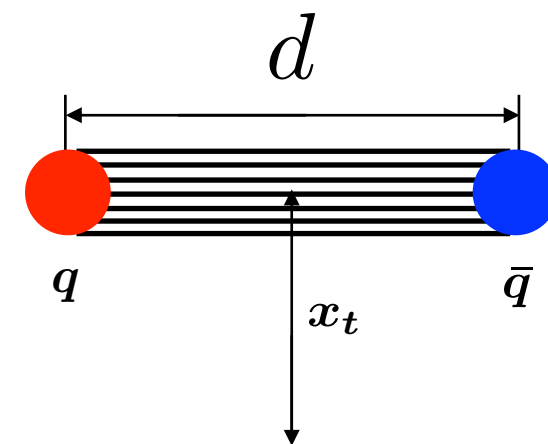
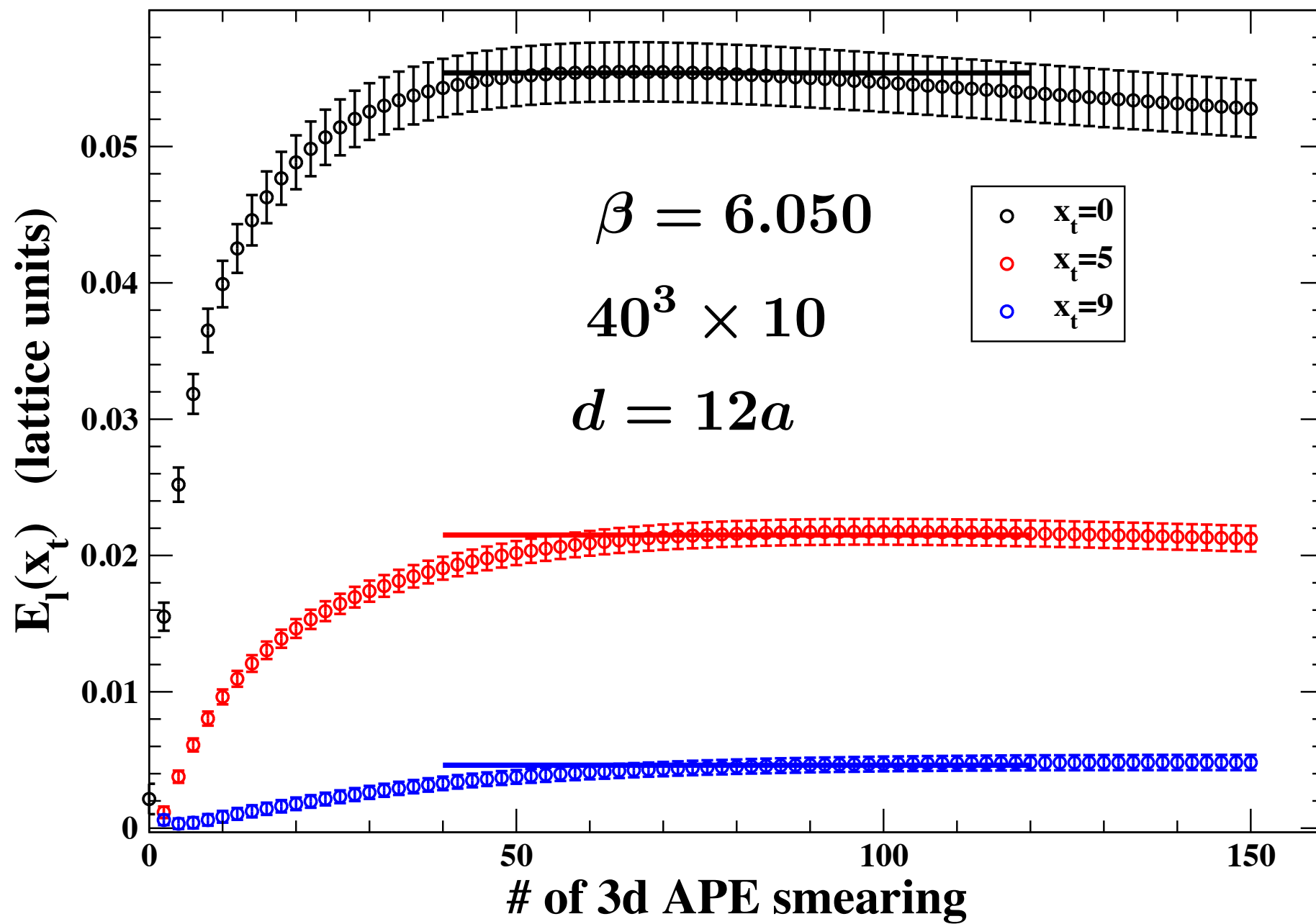
$$\hat{a}(g) = \frac{f_{\text{SU}(3)}(g^2)}{f_{\text{SU}(3)}(g^2(\beta = 6))}$$
$$\beta = \frac{6}{g^2}, \quad 5.6 \leq \beta \leq 6.5$$

$$\sqrt{\sigma} = 420 \text{ MeV}$$

$$f_{\text{SU}(3)}(g^2) = (b_0 g^2)^{-b_1/2b_0^2} \exp\left(-\frac{1}{2b_0 g^2}\right) \quad b_0 = \frac{11}{(4\pi)^2}, \quad b_1 = \frac{102}{(4\pi)^4}$$

- # of measurements for each value of the gauge coupling: 3k to 8k (every 10 trajectories)
- **MILC** code (suitably modified to measure the chromoelectric field)

SMOOTHING OF THE GAUGE CONFIGURATIONS



DATA

$$T_c = 260 \text{ MeV} \quad T = \frac{1}{a(\beta) N_t}$$

$$a(\beta) = \frac{1}{T_c} \frac{1}{\frac{T}{T_c} N_t} = \frac{197 \text{ MeV fm}}{260 \text{ MeV}} \frac{1}{\frac{T}{T_c} N_t}$$

$d \simeq 0.76 \text{ fm}$

N_s	N_t	beta	a (fm)	distance (lattice)	distance (fm)	T/T_c
32	32	6.050	0.0952	8	0.761	0.00
40	10	6.050	0.0952	8	0.761	0.80
40	10	6.125	0.0846	9	0.762	0.90
40	10	6.200	0.0756	10	0.756	1.00
40	10	6.265	0.0689	11	0.757	1.10
40	10	6.325	0.0633	12	0.759	1.20
64	16	6.370	0.0595	13	0.773	0.80

$d \simeq 0.95 \text{ fm}$

N_s	N_t	beta	a (fm)	distance (lattice)	distance (fm)	T/T_c
32	32	6.050	0.0952	10	0.952	0.00
40	10	6.050	0.0952	10	0.952	0.80
40	10	6.125	0.0846	11	0.931	0.90
40	10	6.200	0.0756	13	0.983	1.00
40	10	6.265	0.0689	14	0.964	1.10
40	10	6.325	0.0633	15	0.949	1.20

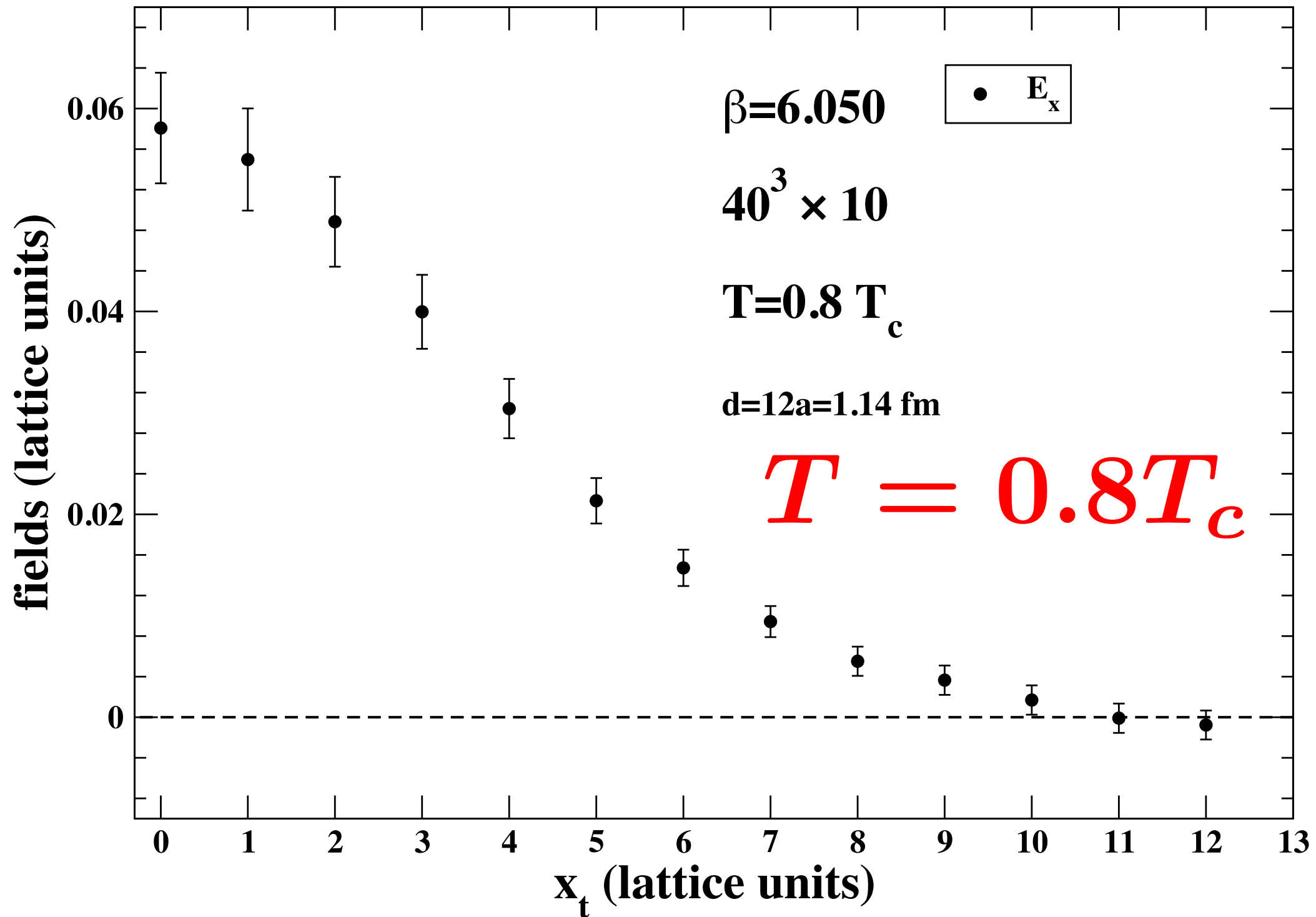
$d \simeq 1.14 \text{ fm}$

N_s	N_t	beta	a (fm)	distance (lattice)	distance (fm)	T/T_c
32	32	6.050	0.0952	12	1.142	0.00
40	10	6.050	0.0952	12	1.142	0.80
40	10	6.125	0.0846	14	1.185	0.90
40	10	6.200	0.0756	15	1.135	1.00
40	10	6.265	0.0689	17	1.171	1.10
40	10	6.325	0.0633	18	1.139	1.20
48	8	6.325	0.0633	18	1.139	1.50
48	12	6.170	0.0791	14	1.107	0.80

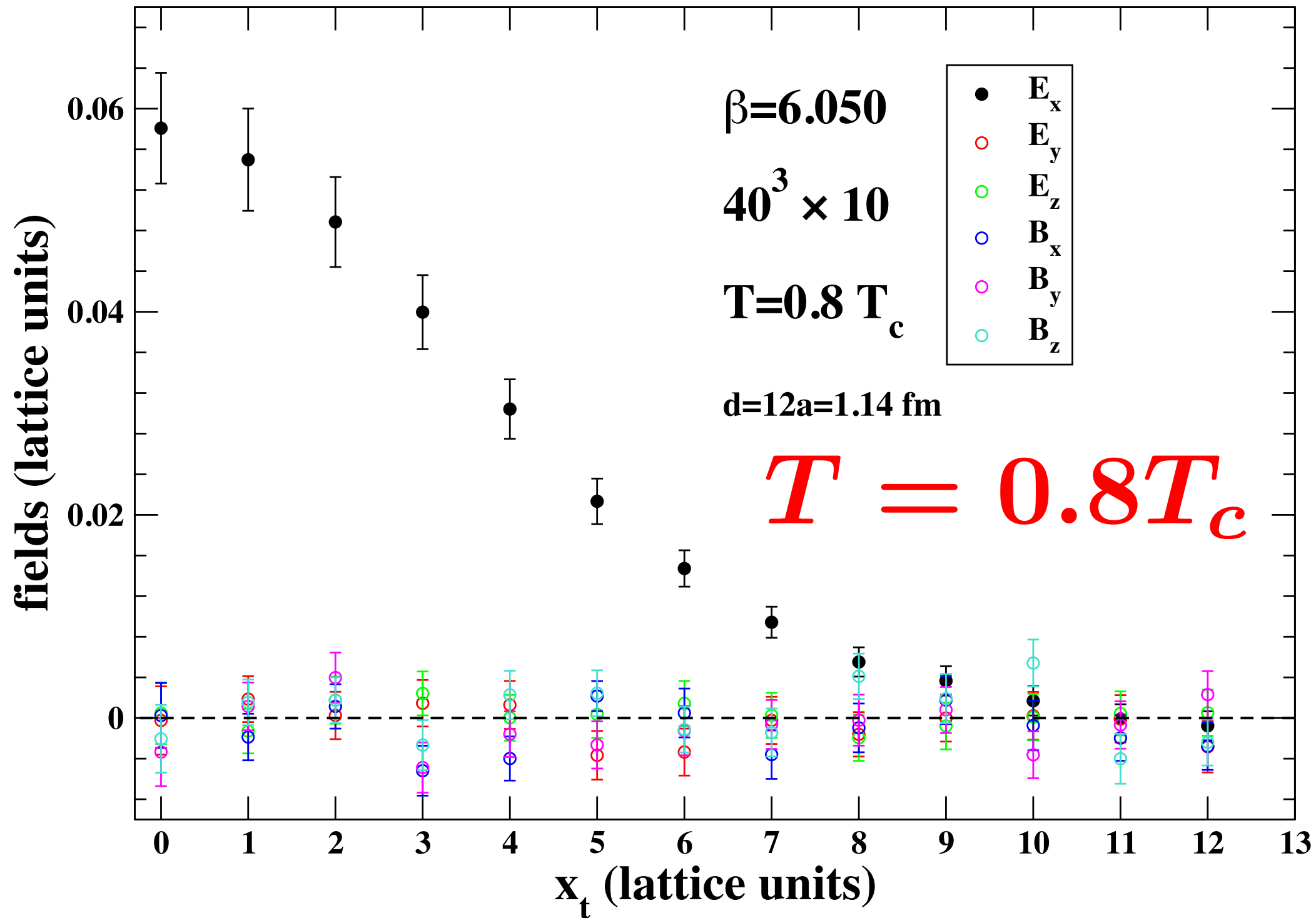
$d \simeq 1.33 \text{ fm}$

N_s	N_t	beta	a (fm)	distance (lattice)	distance (fm)	T/T_c
32	32	6.050	0.0952	14	1.332	0.00
40	10	6.052	0.0949	14	1.328	0.80
40	10	6.127	0.0844	16	1.350	0.90
40	10	6.198	0.0759	18	1.366	1.00
40	10	6.264	0.0690	19	1.310	1.10
48	8	6.170	0.0791	17	1.344	1.20
64	16	6.372	0.0593	23	1.364	0.80

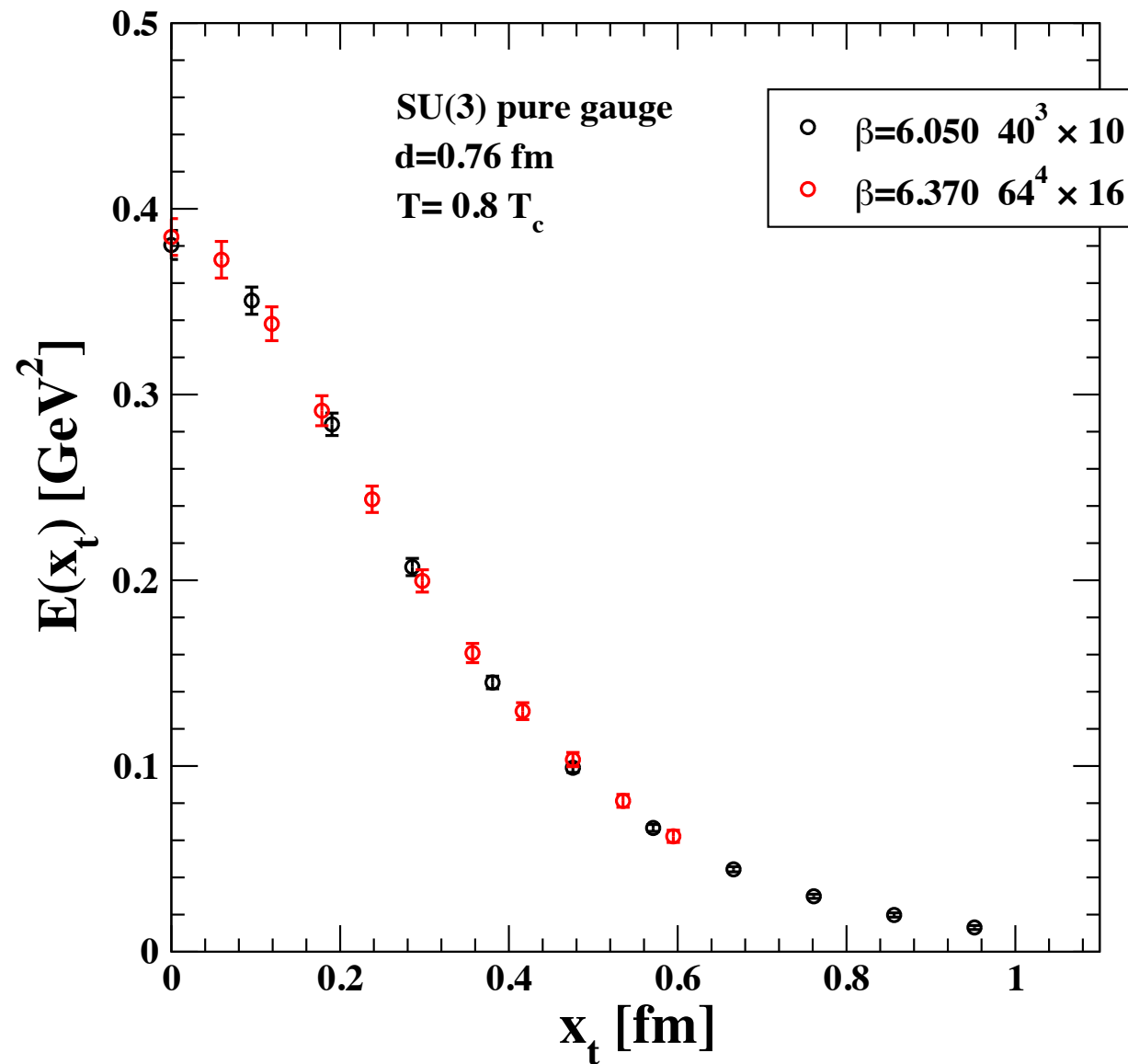
The flux tube is almost completely formed by the longitudinal chromoelectric field



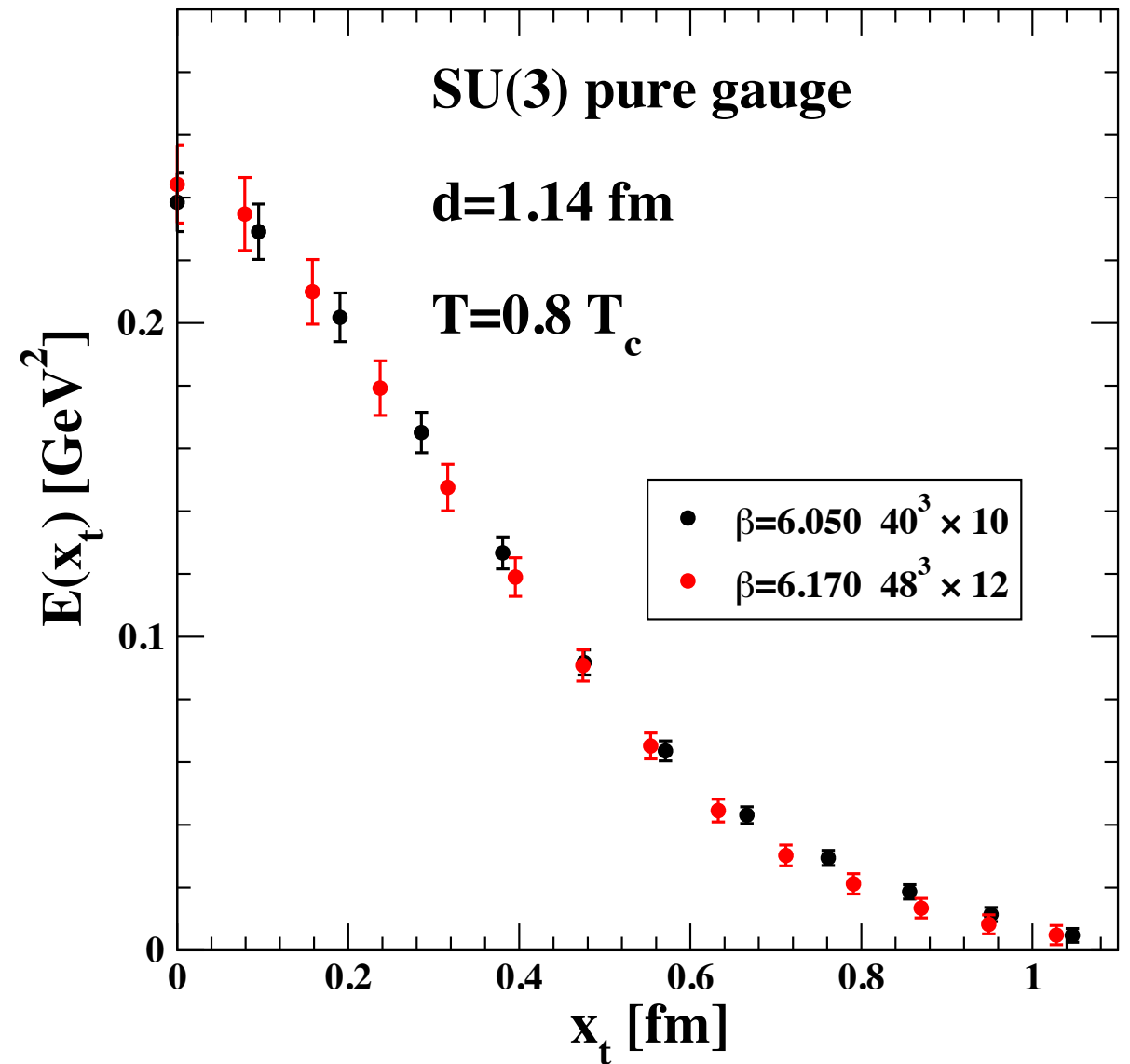
The flux tube is almost completely formed by the longitudinal chromoelectric field



check continuum scaling

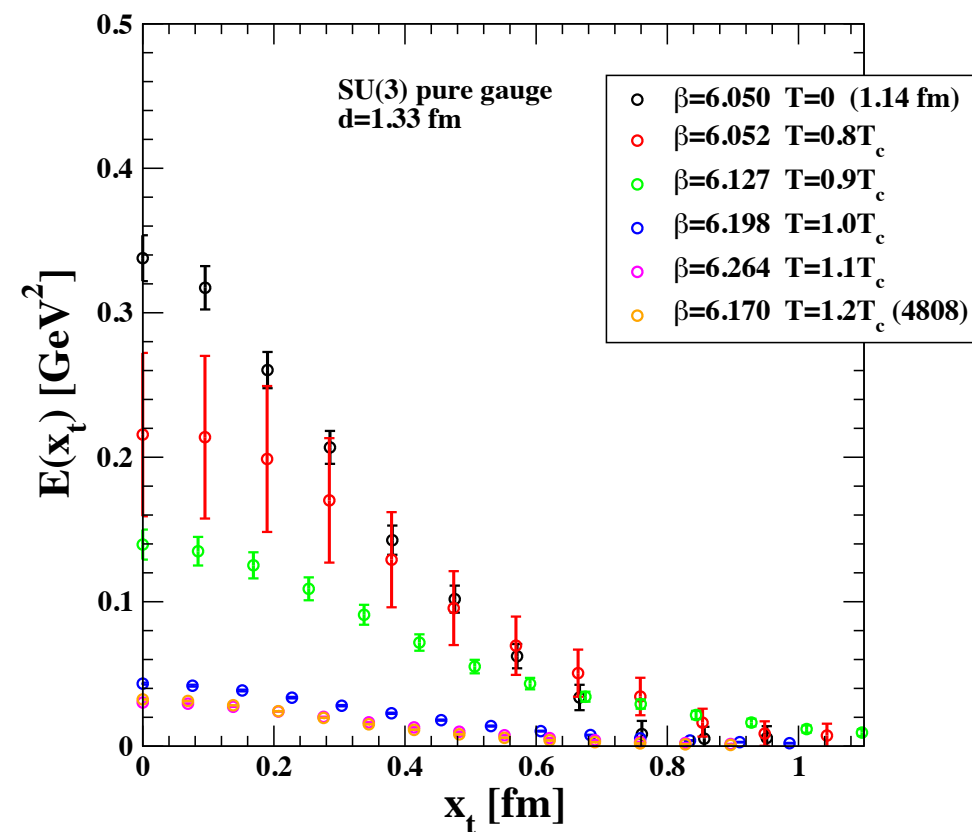
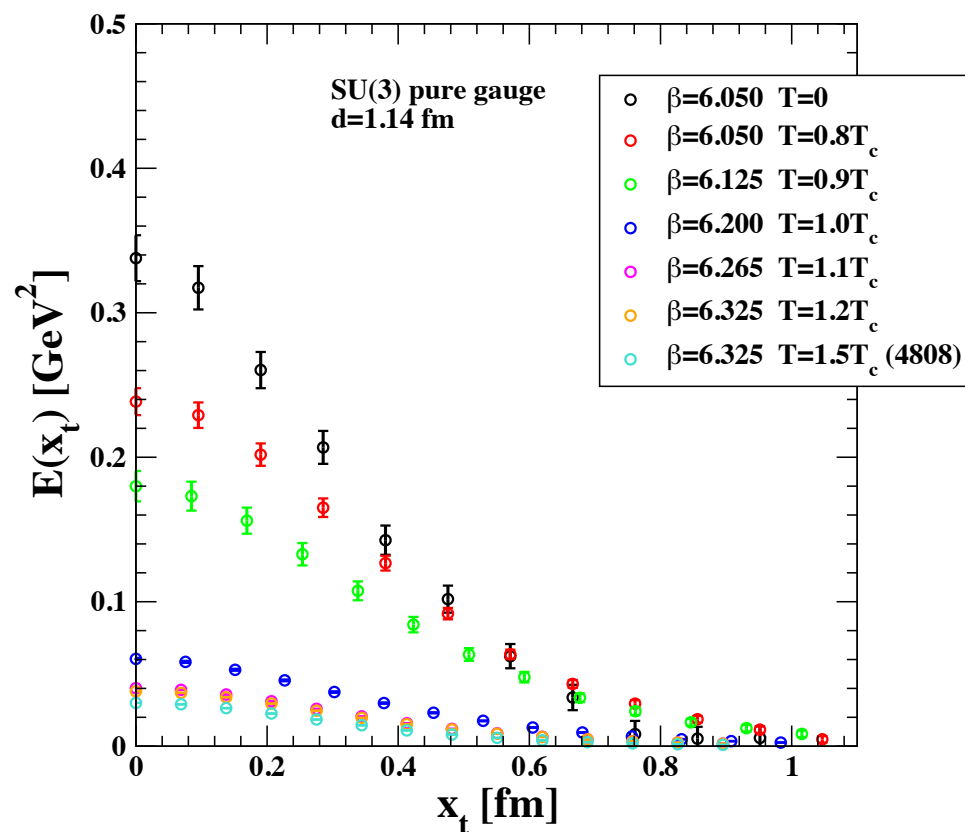
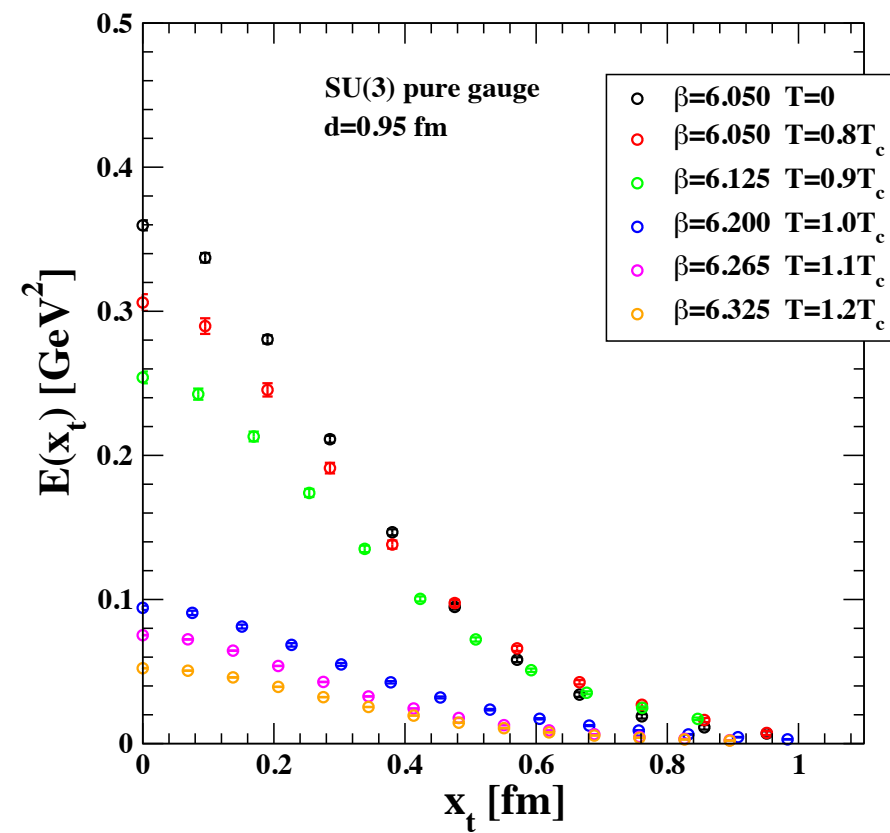
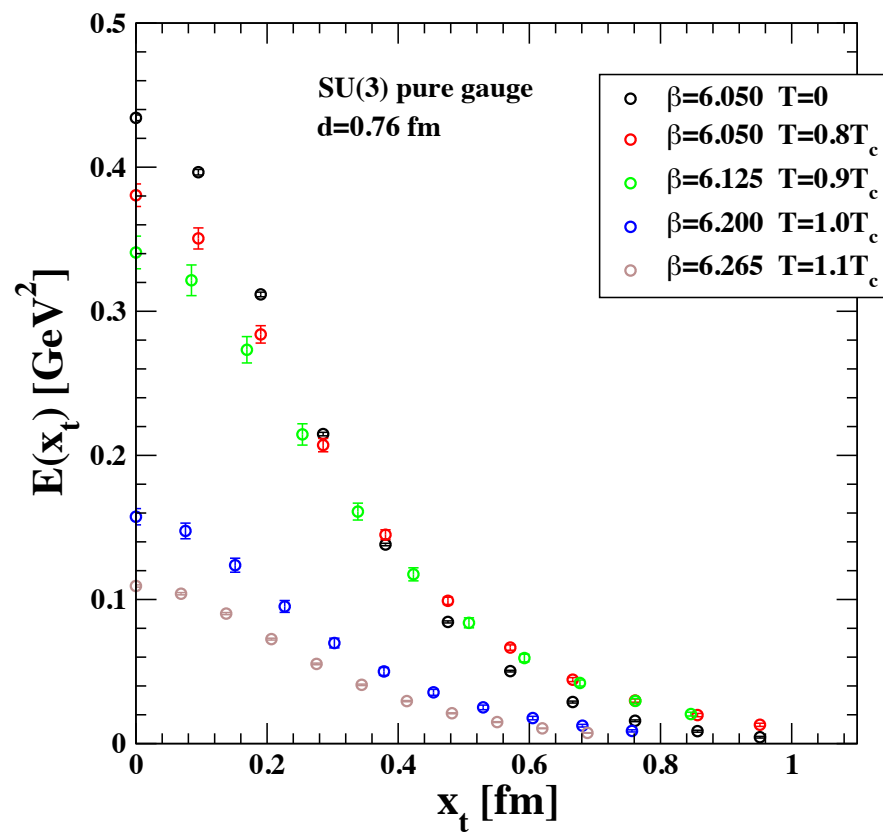


- The continuum scaling is reached at least for $\beta=6.050$



- The smoothing procedure is robust: if the smearing had corrupted the physical signal it would be quite unlikely to obtain such a nice scaling

the longitudinal field across deconfinement



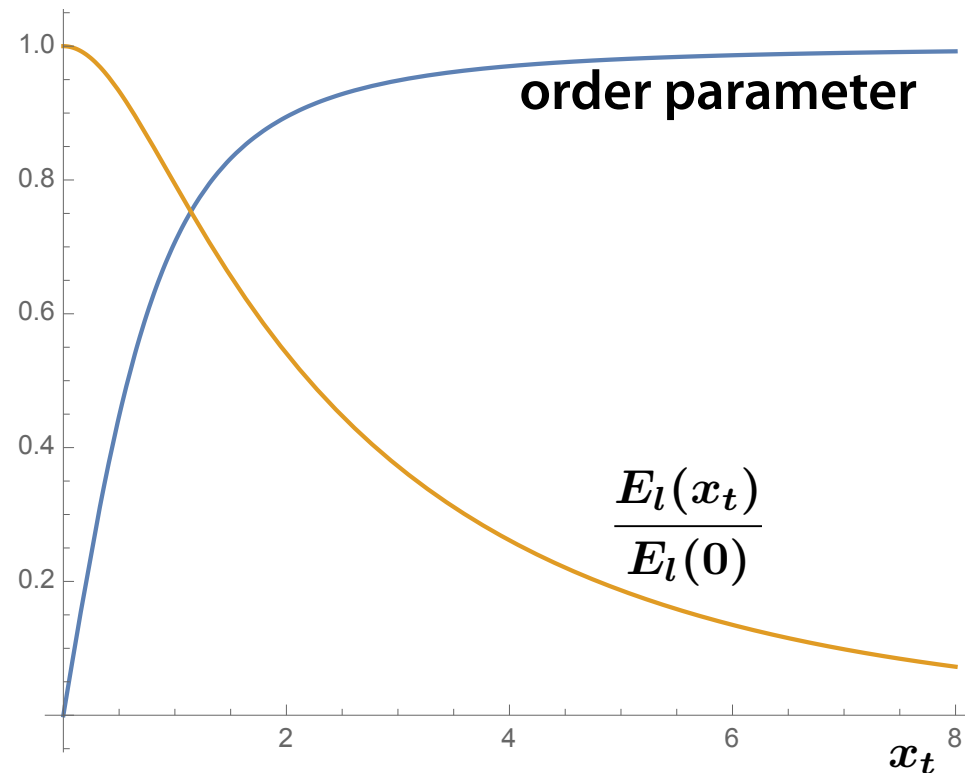
The flux tube shape up to $x_t = 0$

J.R. Clem, J. Low Temp. Phys. 18 (1975) 427

Variational model for the magnitude of the normalised order parameter of an isolated vortex



Analytic expression for the magnetic field and supercurrent density that solve Ampere's law and the Ginzburg-Landau equation.



$$E_l(x_t) = \frac{\phi}{2\pi} \frac{\mu^2}{\alpha} \frac{K_0((\mu^2 x_t^2 + \alpha^2)^{1/2})}{K_1(\alpha)}$$

$$\mu = \frac{1}{\lambda}, \quad \frac{1}{\alpha} = \frac{\lambda}{\xi_v}$$

λ London penetration length

ξ_v variational core radius

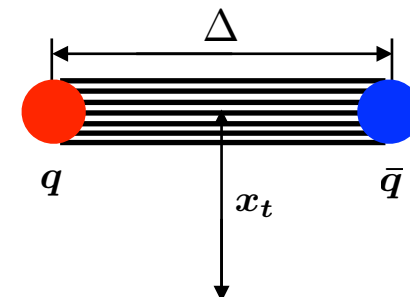
ξ coherence length

κ Ginzburg – Landau parameter

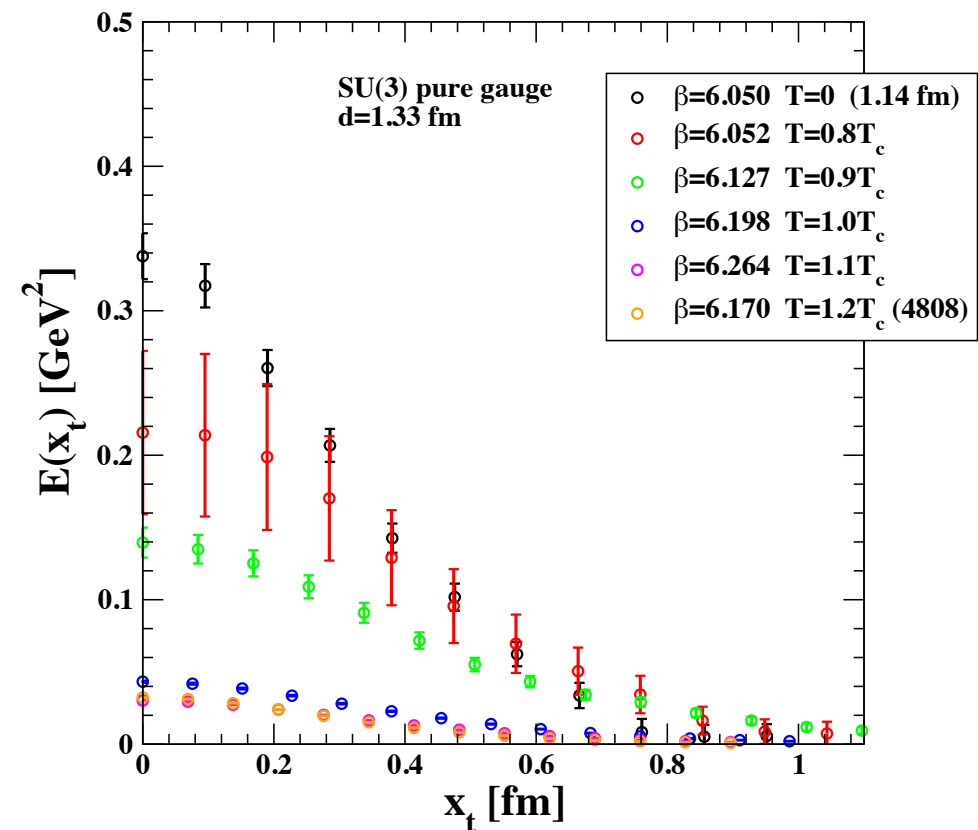
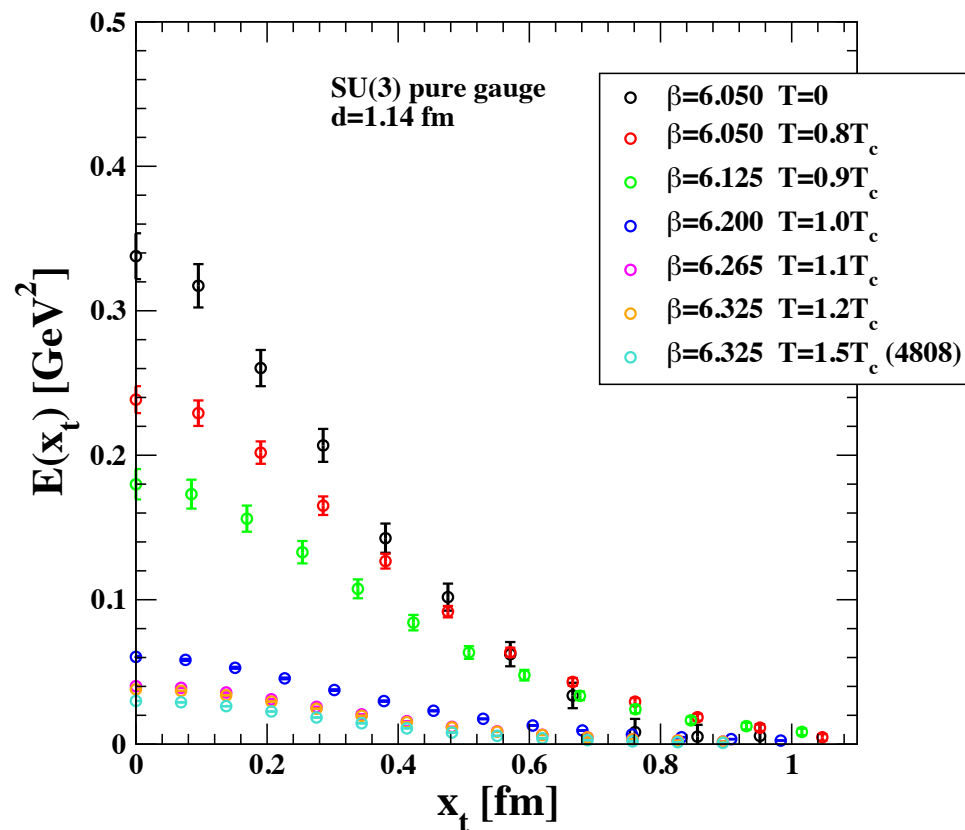
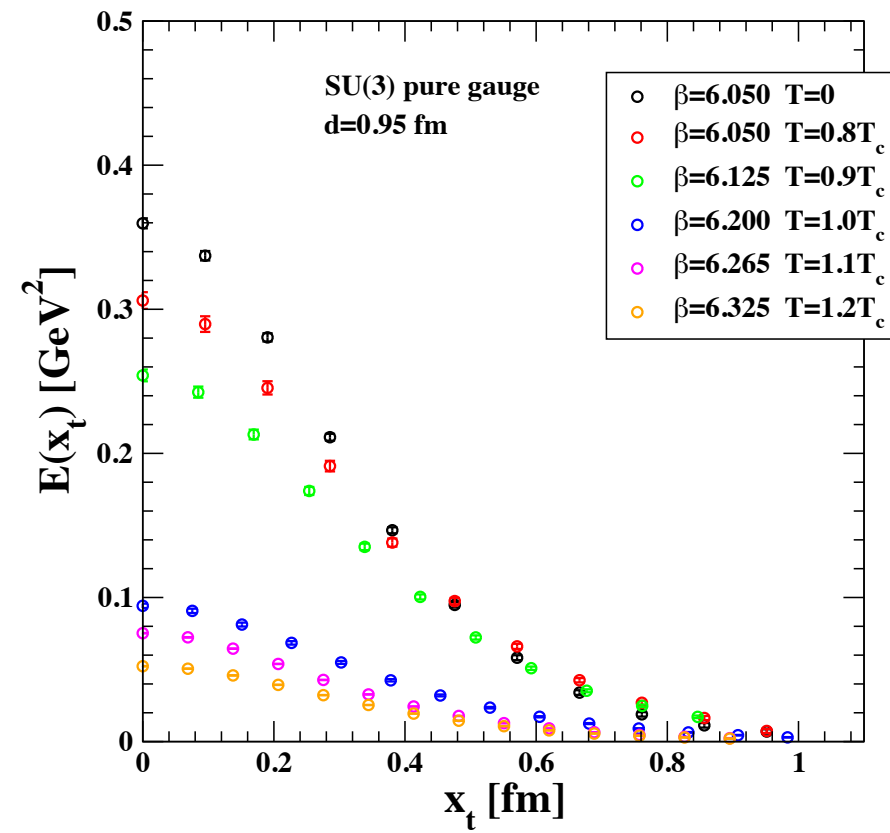
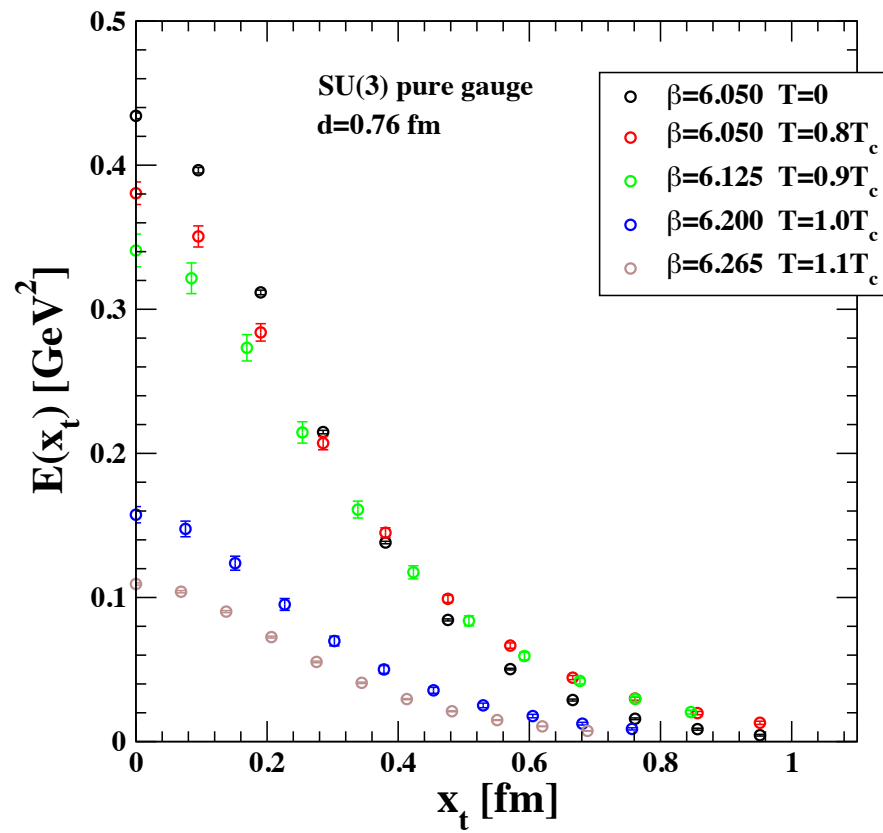
$$\kappa = \frac{\lambda}{\xi} = \frac{\sqrt{2}}{\alpha} [1 - K_0^2(\alpha)/K_1^2(\alpha)]^{1/2}$$

Analyze lattice data for the flux tubes by exploiting the Clem fit analytic expression for the transverse behaviour of the color electric field.

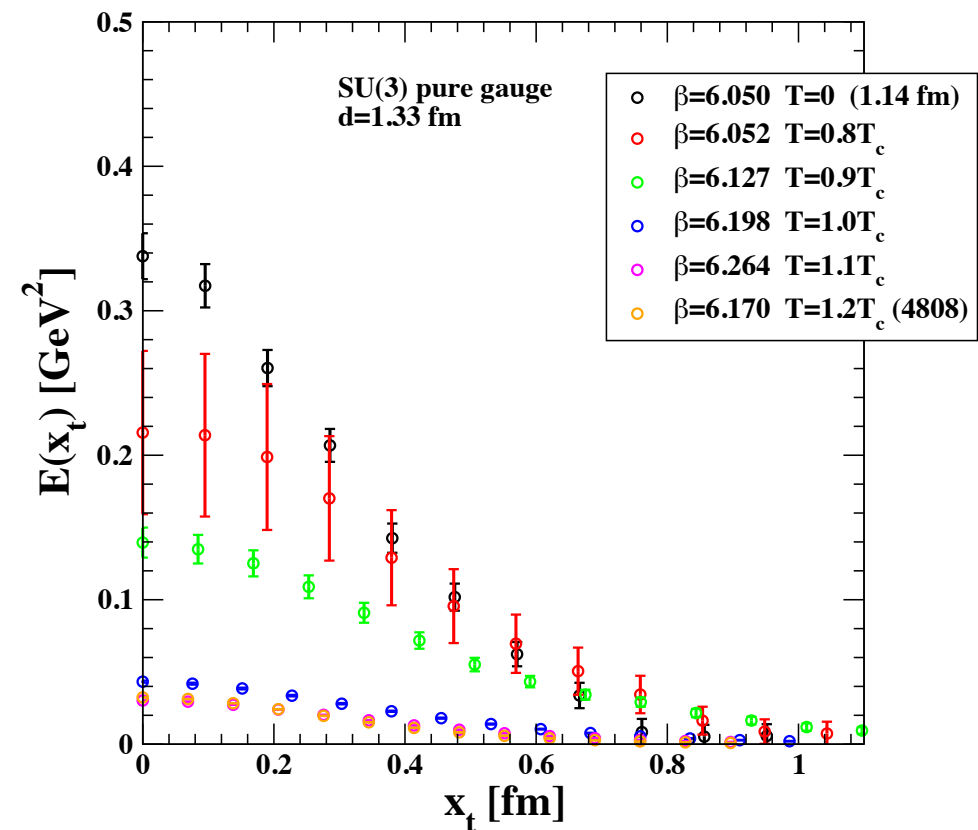
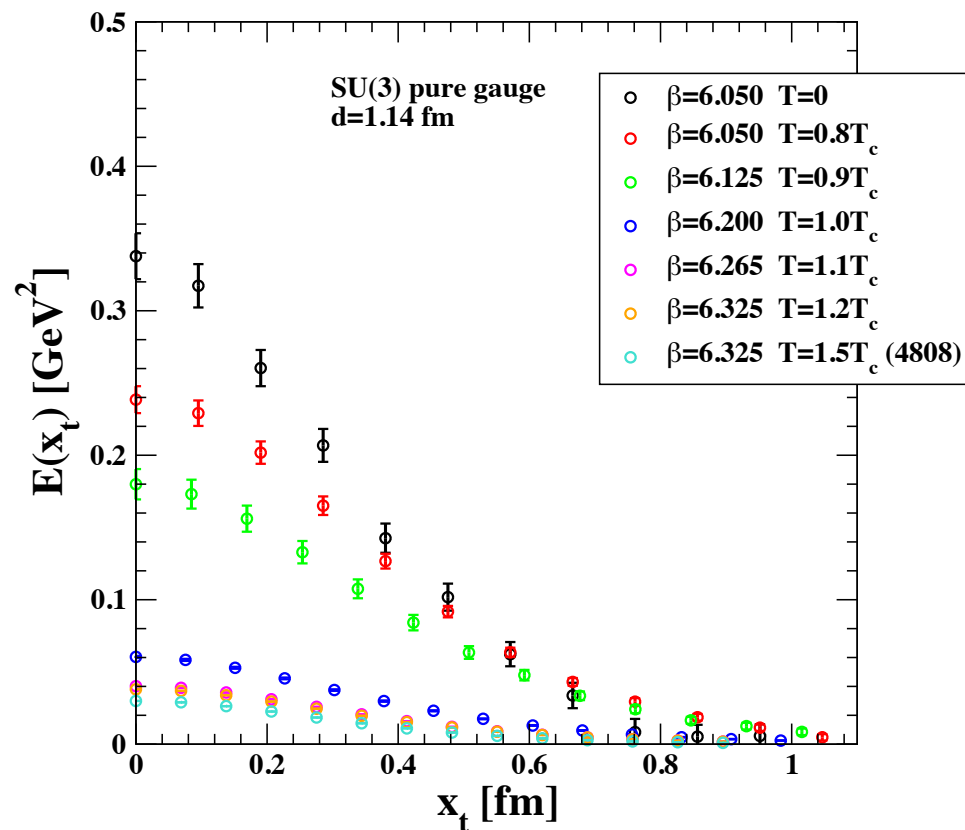
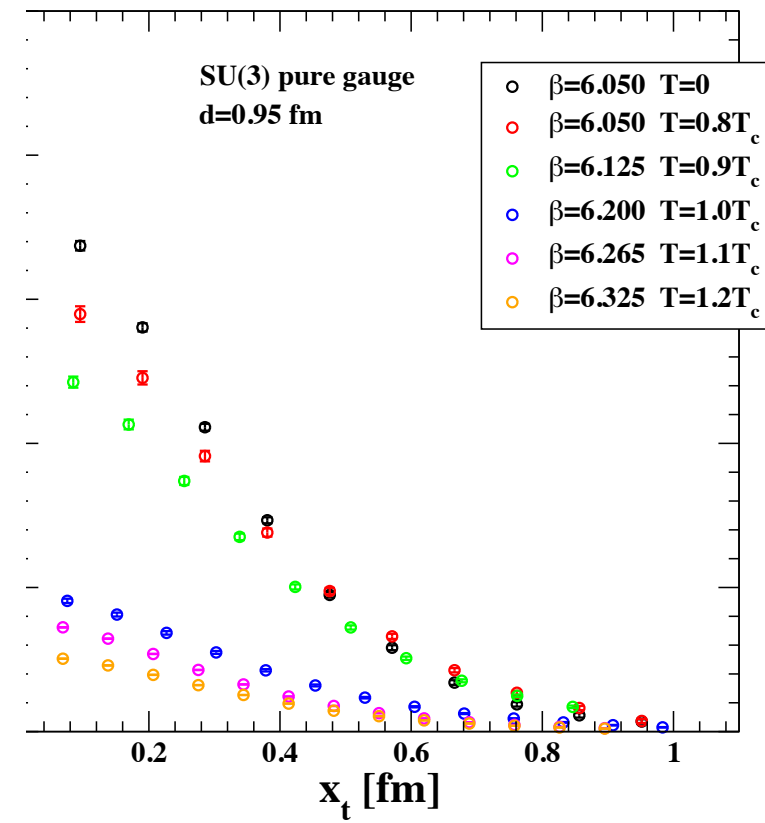
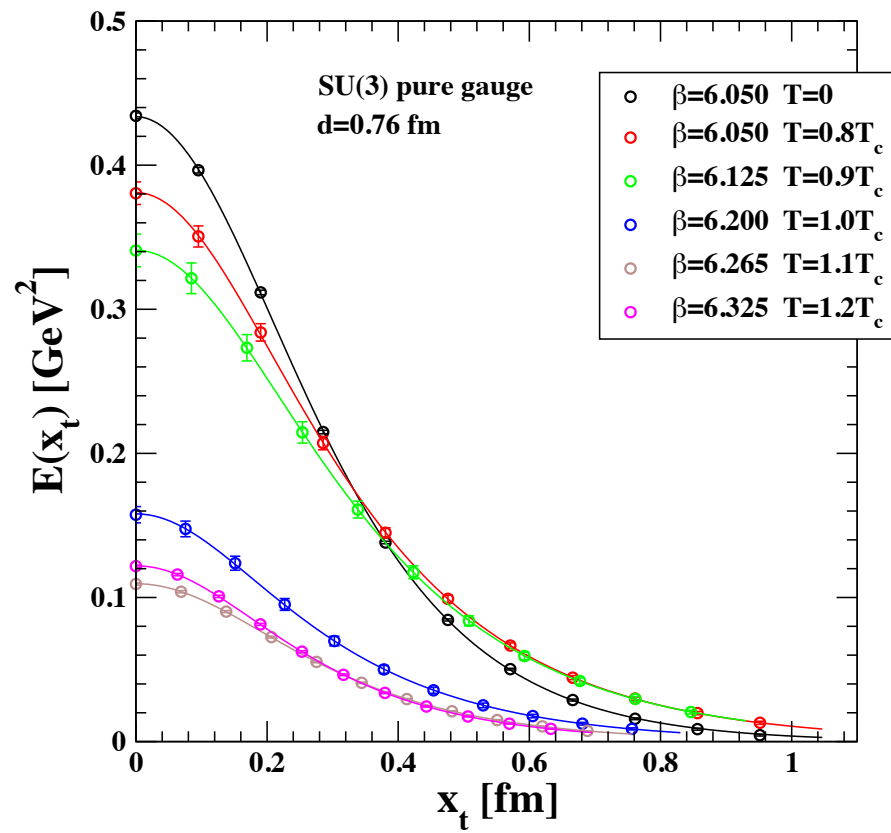
P. Cea, L.C., A.Papa, Phys. Rev. D86 (2012)054501



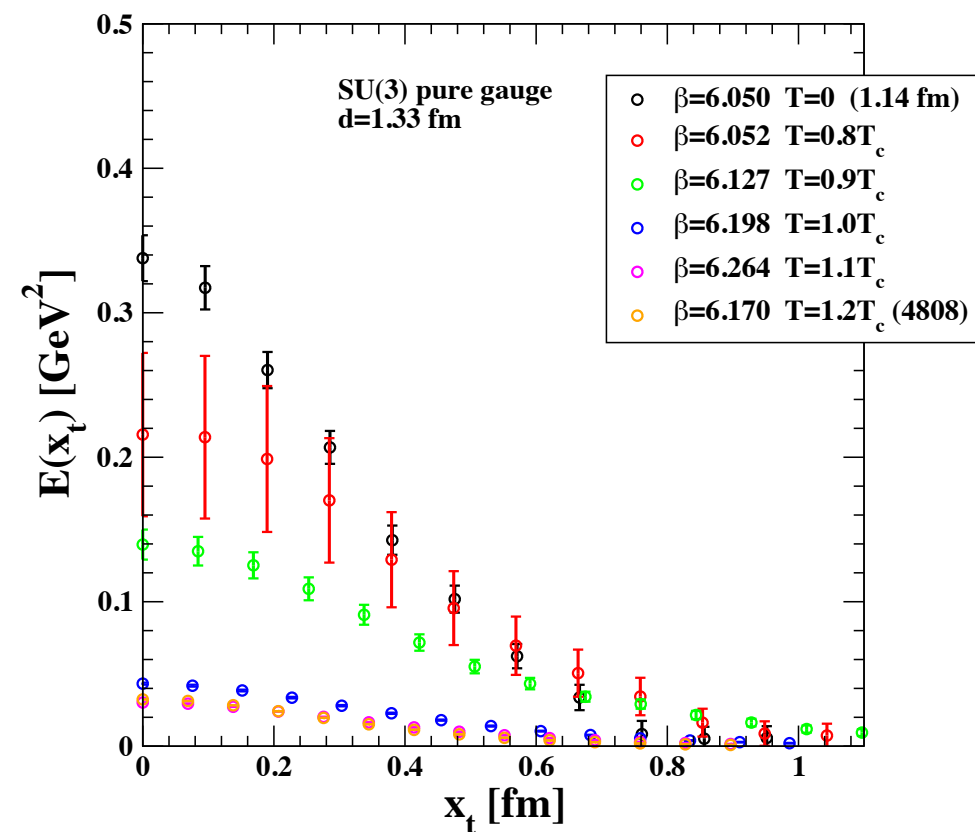
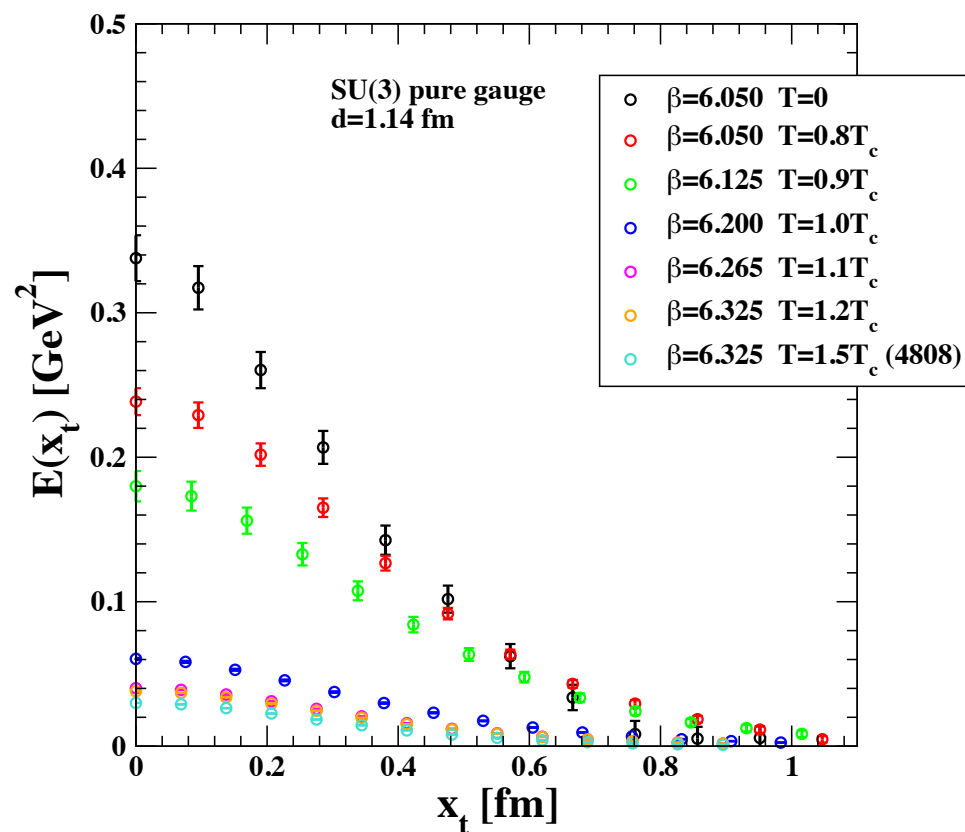
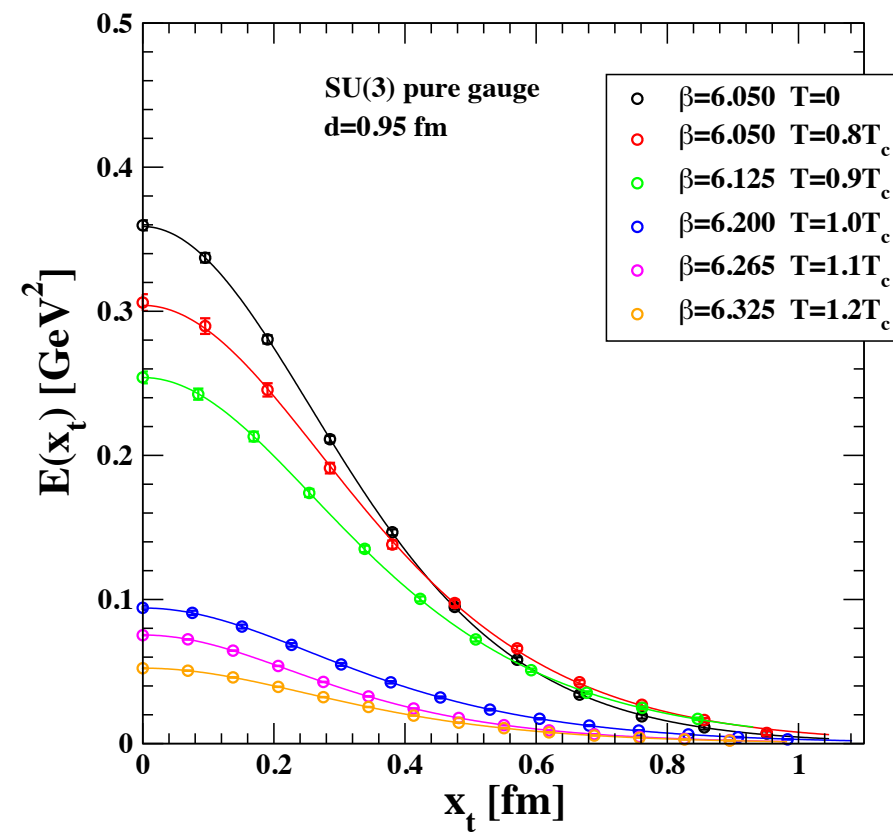
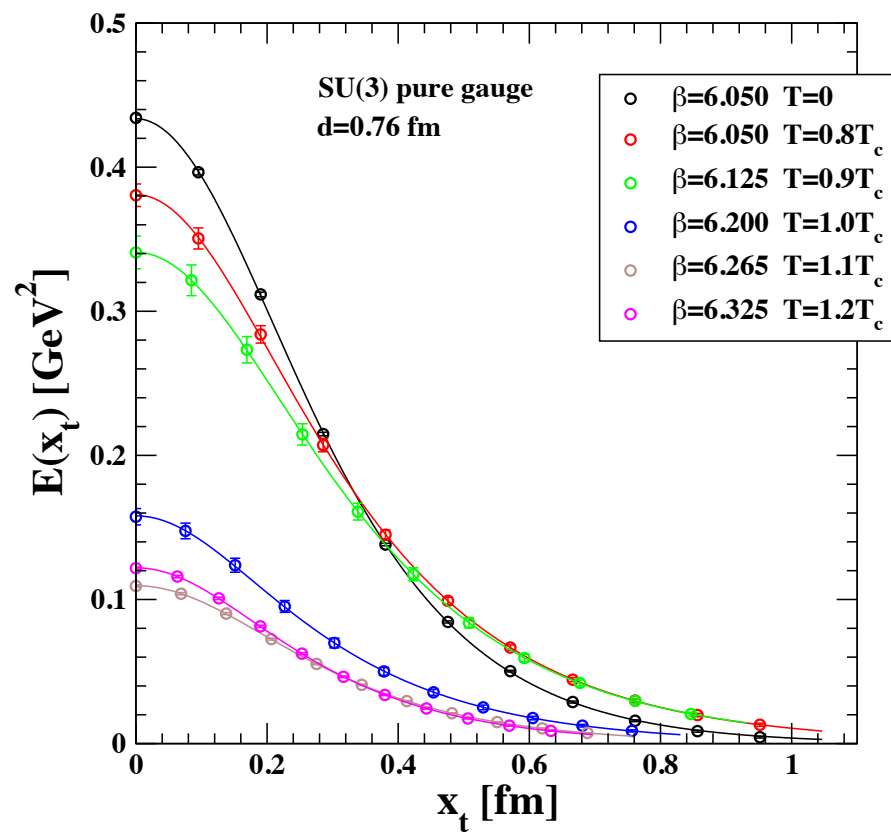
the longitudinal field across deconfinement with Clem fit



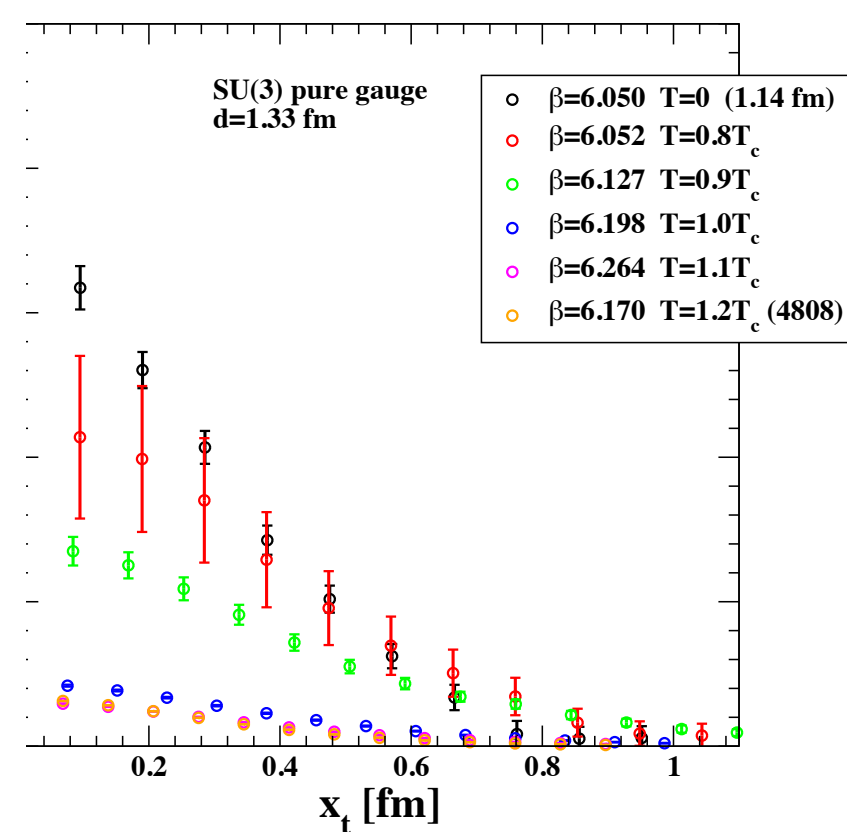
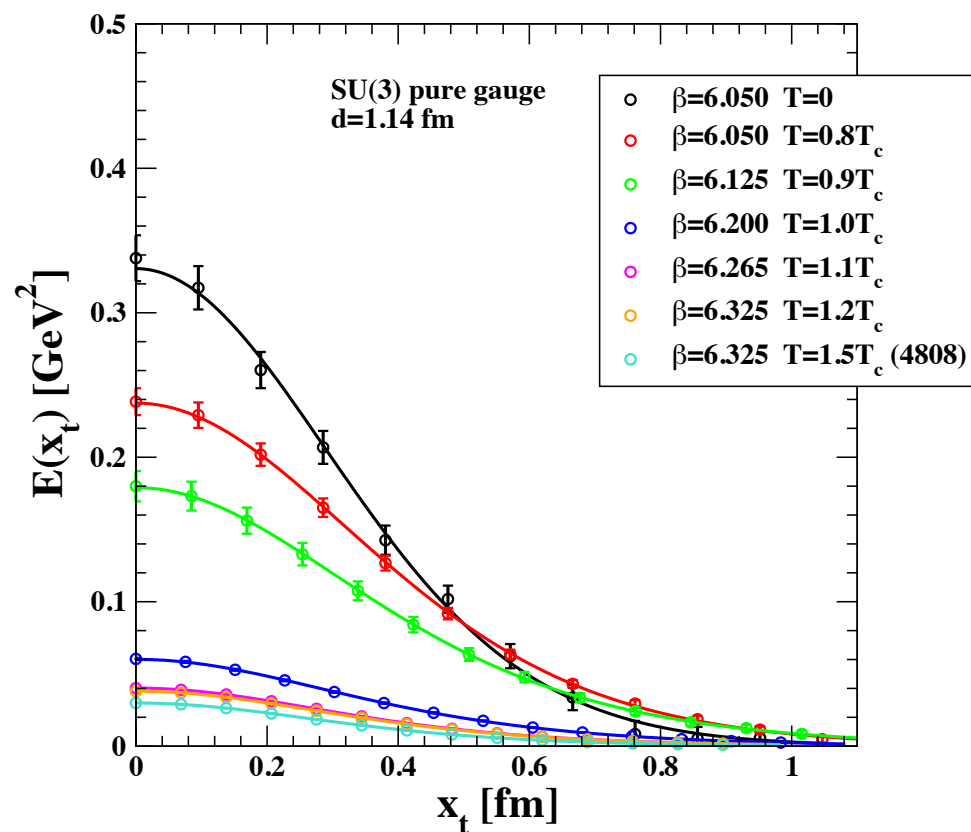
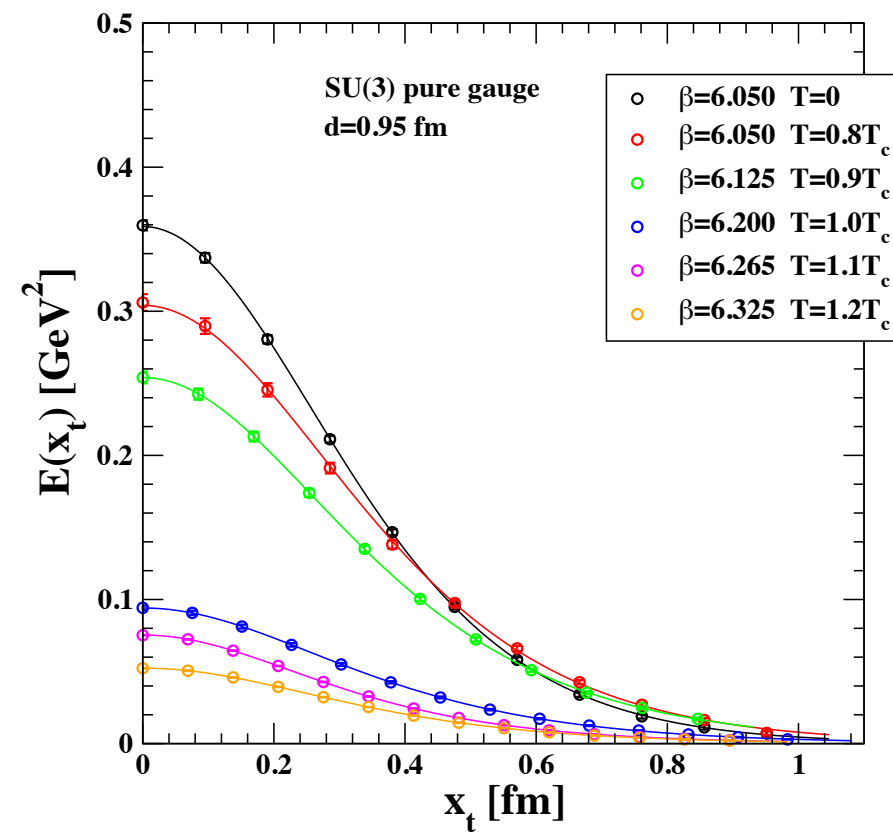
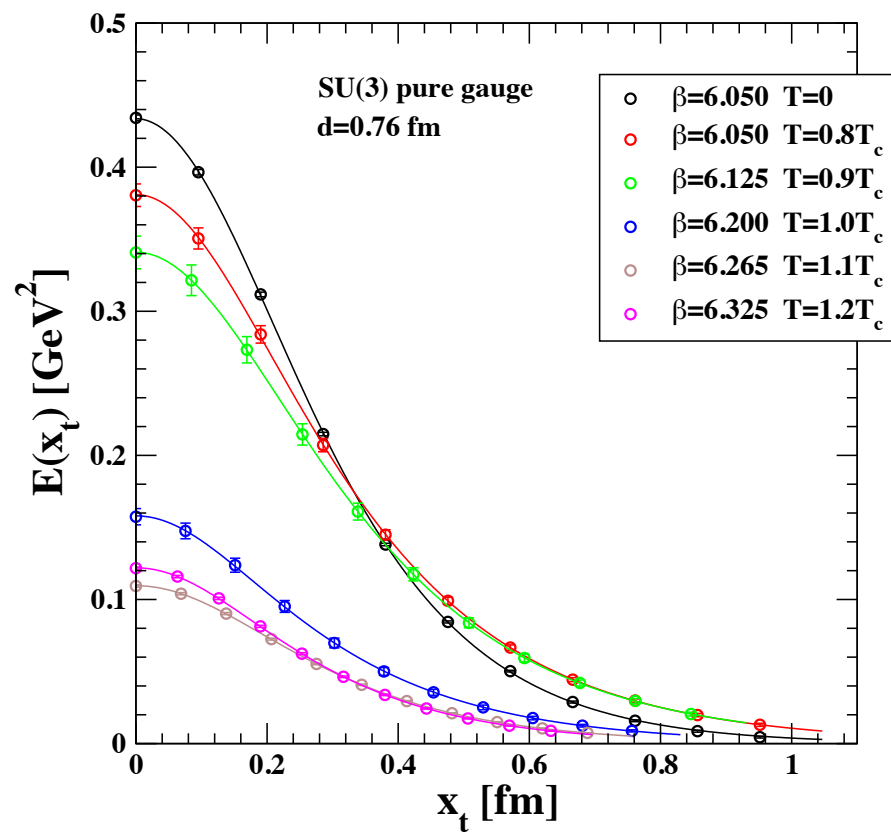
the longitudinal field across deconfinement with Clem fit



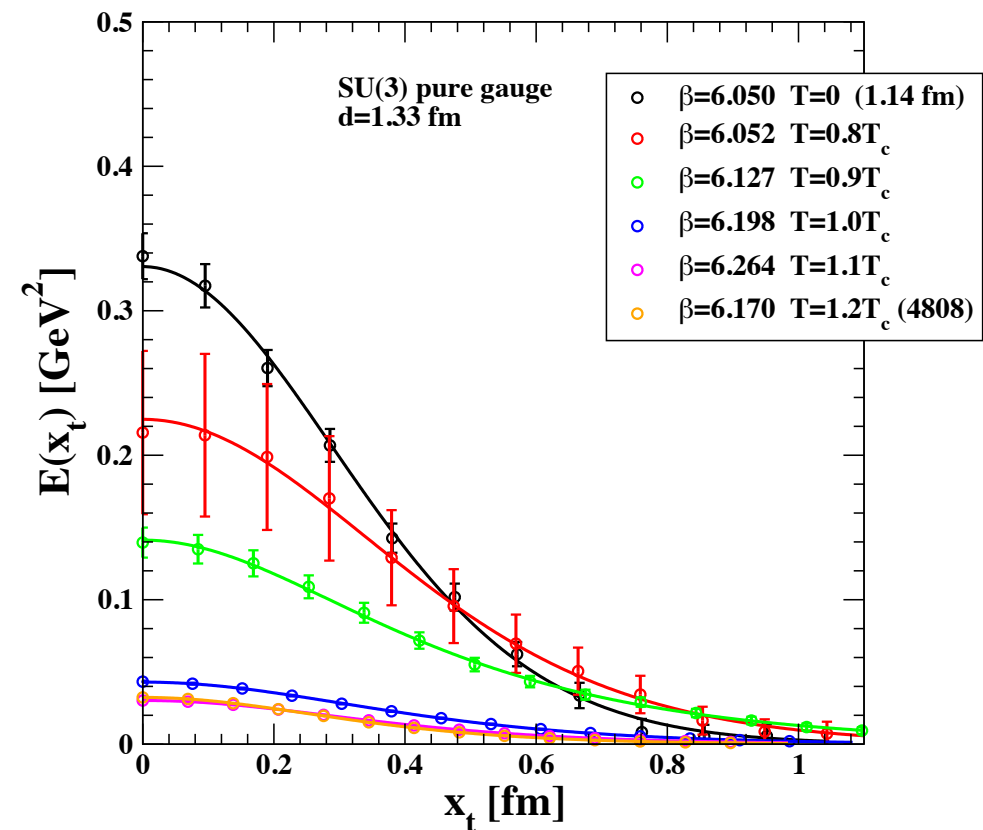
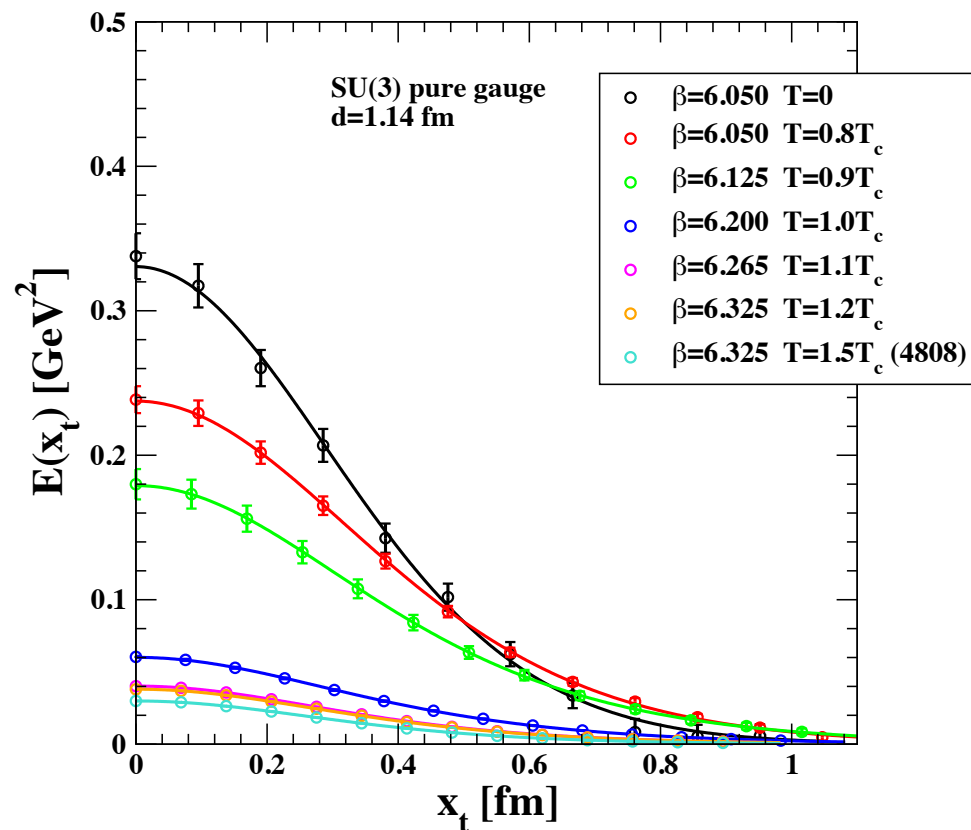
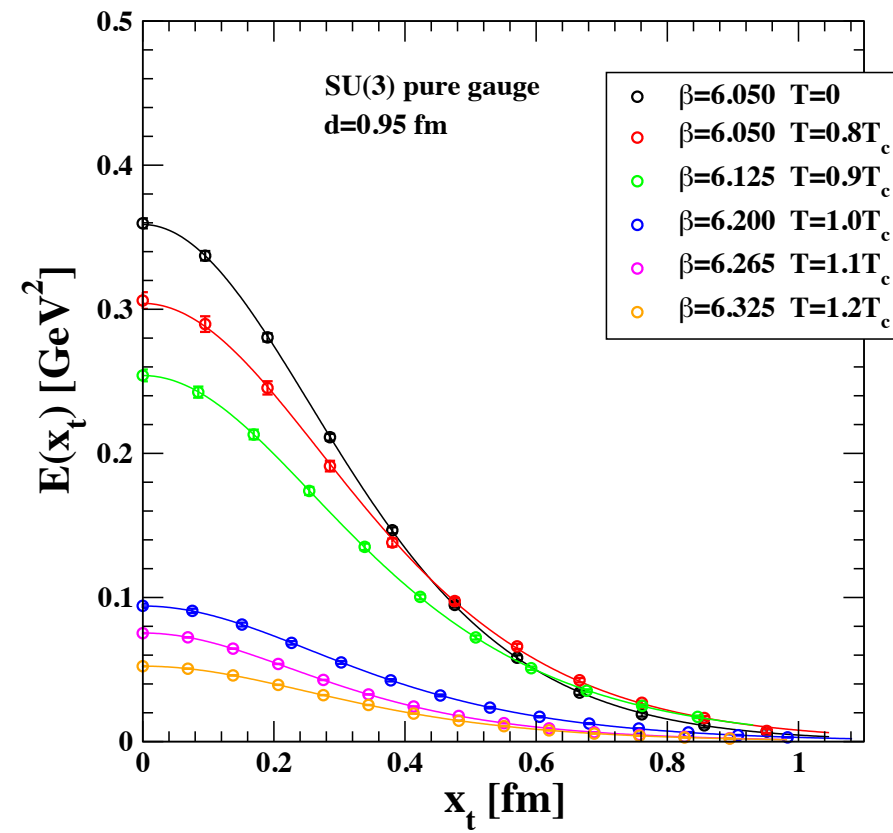
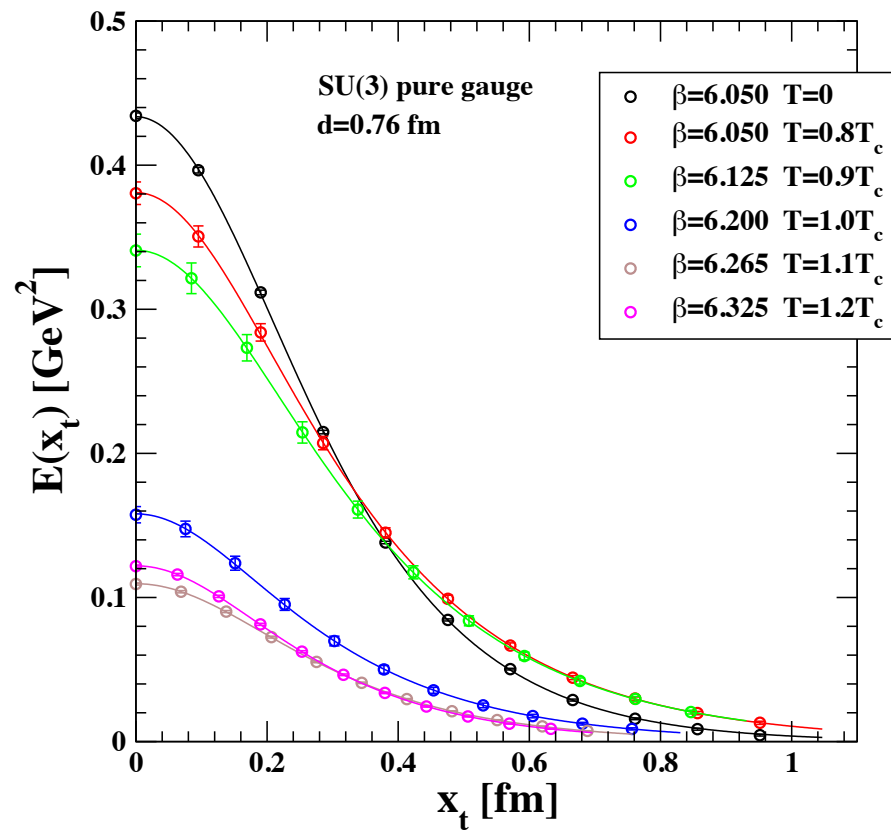
the longitudinal field across deconfinement with Clem fit



the longitudinal field across deconfinement with Clem fit



the longitudinal field across deconfinement with Clem fit



PARAMETERS FROM THE CLEM FIT

L_s	L_t	beta	a (fm)	distance (lattice)	distance (fm)	T/T_c	phi	error	lambda (fm)	error	csi (fm)	error	sqrt(w^2) (fm)	error	sqrt(epsilon)/phi (GeV)	error
32	32	6.050	0.0952	14	1.332232	0.00	5.000	0.292	0.169	0.016	0.715	0.335	0.512	0.114	0.117	0.030
40	10	6.052	0.0949	14	1.327978	0.80	5.317	1.108	0.158	0.267	1.520	2.604	0.589	1.308	0.099	0.229
40	10	6.127	0.0844	16	1.350063	0.90	4.400	0.440	0.344	0.097	0.426	0.473	0.825	0.258	0.078	0.027
40	10	6.198	0.0759	18	1.365672	1.00	0.971	0.023	0.207	0.024	0.798	0.401	0.614	0.086	0.098	0.015
40	10	6.264	0.0690	19	1.310212	1.10	0.583	0.004	0.337	0.025	0.777	0.362	0.563	0.023	0.106	0.005
48	8	6.170	0.0791	17	1.344381	1.20	0.481	0.002	0.181	0.004	0.845	0.364	0.562	0.014	0.106	0.003

L_s	L_t	beta	a (fm)	distance (lattice)	distance (fm)	T/T_c	phi	error	lambda (fm)	error	csi (fm)	error	sqrt(w^2) (fm)	error	sqrt(epsilon)/phi (GeV)	error
32	32	6.050	0.0952	12	1.141913	0.00	5.218	0.371	0.143	0.041	0.983	0.428	0.488	0.140	0.120	0.035
40	10	6.050	0.0952	12	1.141913	0.80	5.111	0.219	0.164	0.050	1.210	0.533	0.571	0.225	0.103	0.043
40	10	6.125	0.0846	14	1.184918	0.90	4.192	0.262	0.221	0.066	0.732	0.454	0.634	0.231	0.095	0.038
40	10	6.200	0.0756	15	1.134721	1.00	1.245	0.019	0.215	0.015	0.639	0.376	0.603	0.050	0.101	0.009
40	10	6.265	0.0689	17	1.170625	1.10	0.708	0.005	0.189	0.005	0.656	0.345	0.547	0.018	0.110	0.004
40	10	6.325	0.0633	18	1.139092	1.20	0.683	0.003	0.178	0.004	0.587	0.320	0.510	0.012	0.119	0.003
48	8	6.325	0.0633	18	1.139092	1.50	0.466	0.001	0.149	0.002	0.688	0.298	0.461	0.009	0.129	0.003
48	12	6.170	0.0791	14	1.107137	0.80	4.750	0.261	0.142	0.068	1.462	0.796	0.538	0.339	0.108	0.071

L_s	L_t	beta	a (fm)	distance (lattice)	distance (fm)	T/T_c	phi	error	lambda (fm)	error	csi (fm)	error	sqrt(w^2) (fm)	error	sqrt(epsilon)/phi (GeV)	error
32	32	6.050	0.0952	10	0.951594	0.00	5.287	0.109	0.146	0.017	0.859	0.331	0.479	0.069	0.123	0.019
40	10	6.050	0.0952	10	0.951594	0.80	5.507	0.132	0.184	0.023	0.722	0.361	0.549	0.084	0.109	0.018
40	10	6.125	0.0846	11	0.931007	0.90	4.838	0.104	0.219	0.019	0.535	0.361	0.591	0.061	0.104	0.061
40	10	6.200	0.0756	13	0.983425	1.00	1.738	0.025	0.217	0.013	0.518	0.354	0.583	0.042	0.106	0.042
40	10	6.265	0.0689	14	0.964044	1.10	1.095	0.005	0.197	0.003	0.440	0.312	0.521	0.009	0.119	0.002
40	10	6.325	0.0633	15	0.949243	1.20	0.868	0.004	0.180	0.004	0.506	0.307	0.499	0.012	0.122	0.003

L_s	L_t	beta	a (fm)	distance (lattice)	distance (fm)	T/T_c	phi	error	lambda (fm)	error	csi (fm)	error	sqrt(w^2) (fm)	error	sqrt(epsilon)/phi (GeV)	error
32	32	6.050	0.0952	8	0.761275	0.00	5.143	0.039	0.164	0.005	0.472	0.283	0.458	0.017	0.133	0.005
40	10	6.050	0.0952	8	0.761275	0.80	6.201	0.129	0.249	0.017	0.308	0.331	0.596	0.045	0.108	0.009
40	10	6.125	0.0846	9	0.761733	0.90	5.941	0.194	0.251	0.028	0.337	0.344	0.610	0.077	0.105	0.015
40	10	6.200	0.0756	10	0.756481	1.00	2.061	0.086	0.231	0.029	0.253	0.298	0.543	0.076	0.119	0.076
40	10	6.265	0.0689	11	0.757463	1.10	1.359	0.017	0.200	0.008	0.326	0.289	0.501	0.023	0.126	0.006
40	10	6.325	0.0633	12	0.759395	1.20	1.324	0.020	0.190	0.009	0.293	0.270	0.472	0.024	0.134	0.024
64	16	6.370	0.0595	13	0.773170	0.80	6.554	0.490	0.271	0.046	0.271	0.342	0.631	0.115	0.104	0.021

width of the flux tube:

$$\sqrt{w^2} = \sqrt{\frac{\int d^2x_t x_t^2 E_l(x_t)}{\int d^2x_t E_l(x_t)}} = \sqrt{\frac{2\alpha K_2(\alpha)}{\mu^2 K_1(\alpha)}}$$

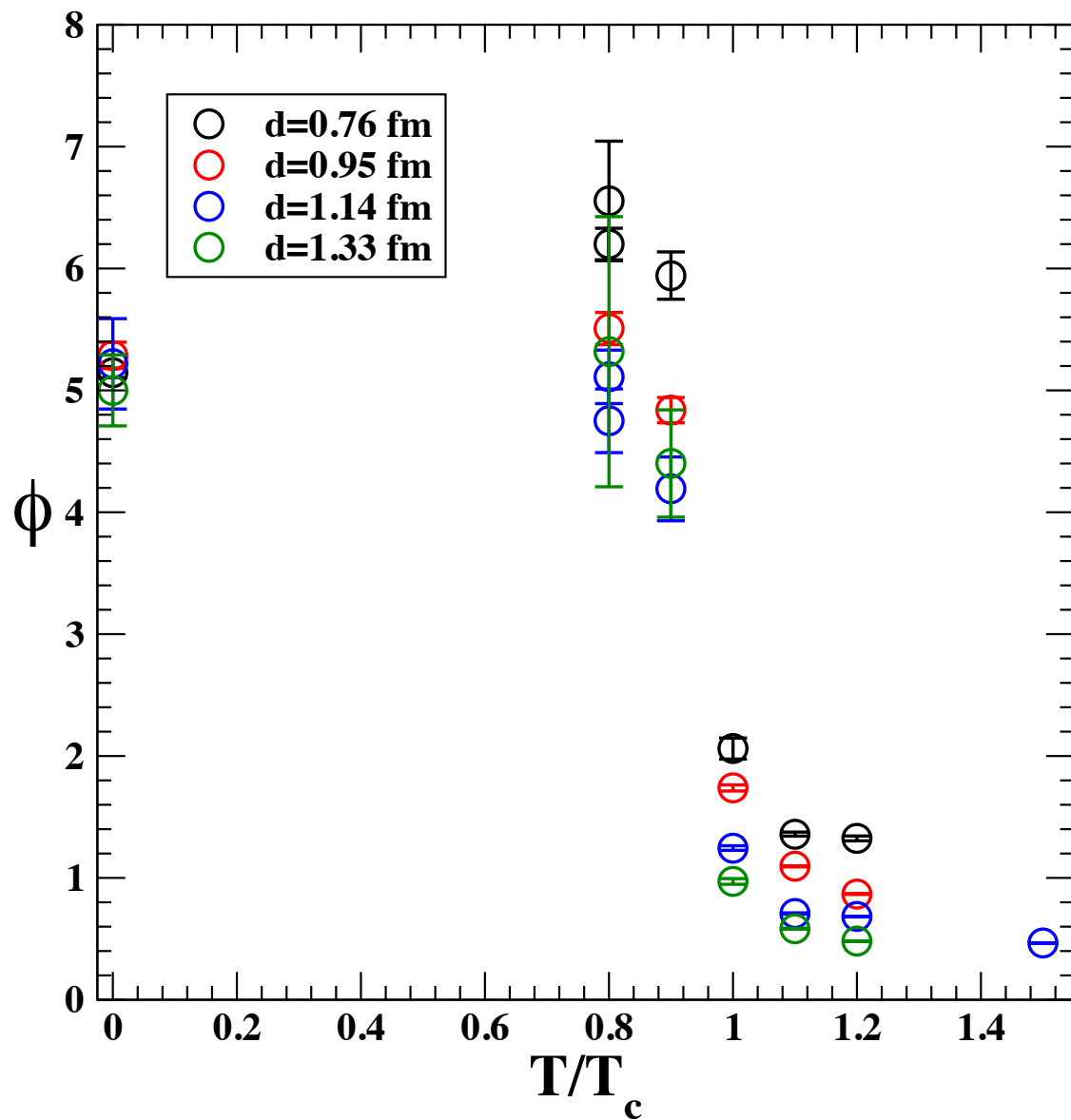
energy in the flux tube per unit length:

$$\varepsilon = \int d^2x_t \frac{E_l(x_t)^2}{2} = \frac{\phi^2}{8\pi} \mu^2 \left(1 - \left(\frac{K_0(\alpha)}{K_1(\alpha)} \right)^2 \right)$$

$$\frac{\sqrt{\varepsilon}}{\phi} = \sqrt{\frac{\mu^2}{8\pi} \left(1 - \left(\frac{K_0(\alpha)}{K_1(\alpha)} \right)^2 \right)}$$

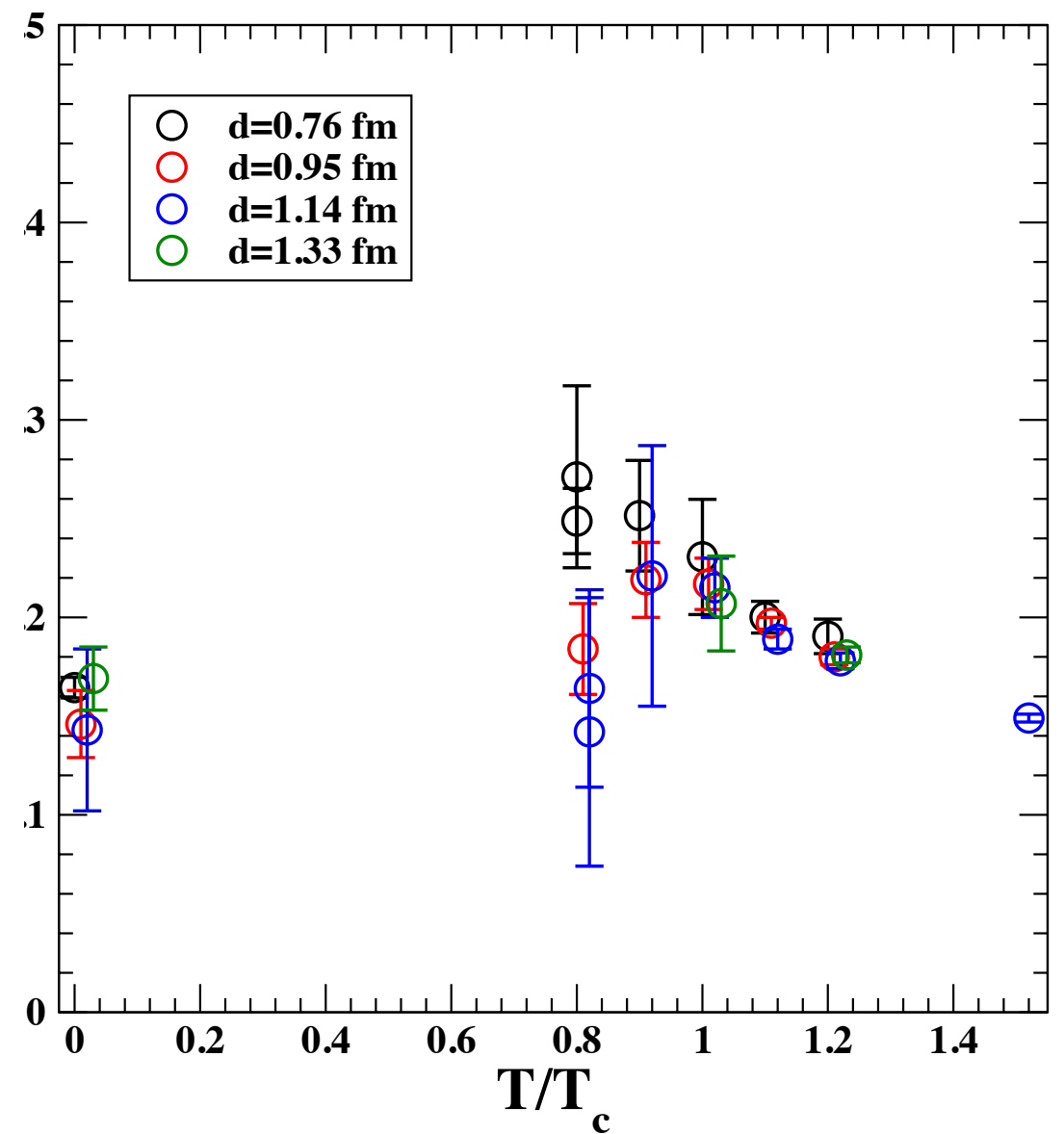
across deconfinement

ϕ



phi drops down across the phase transition

λ

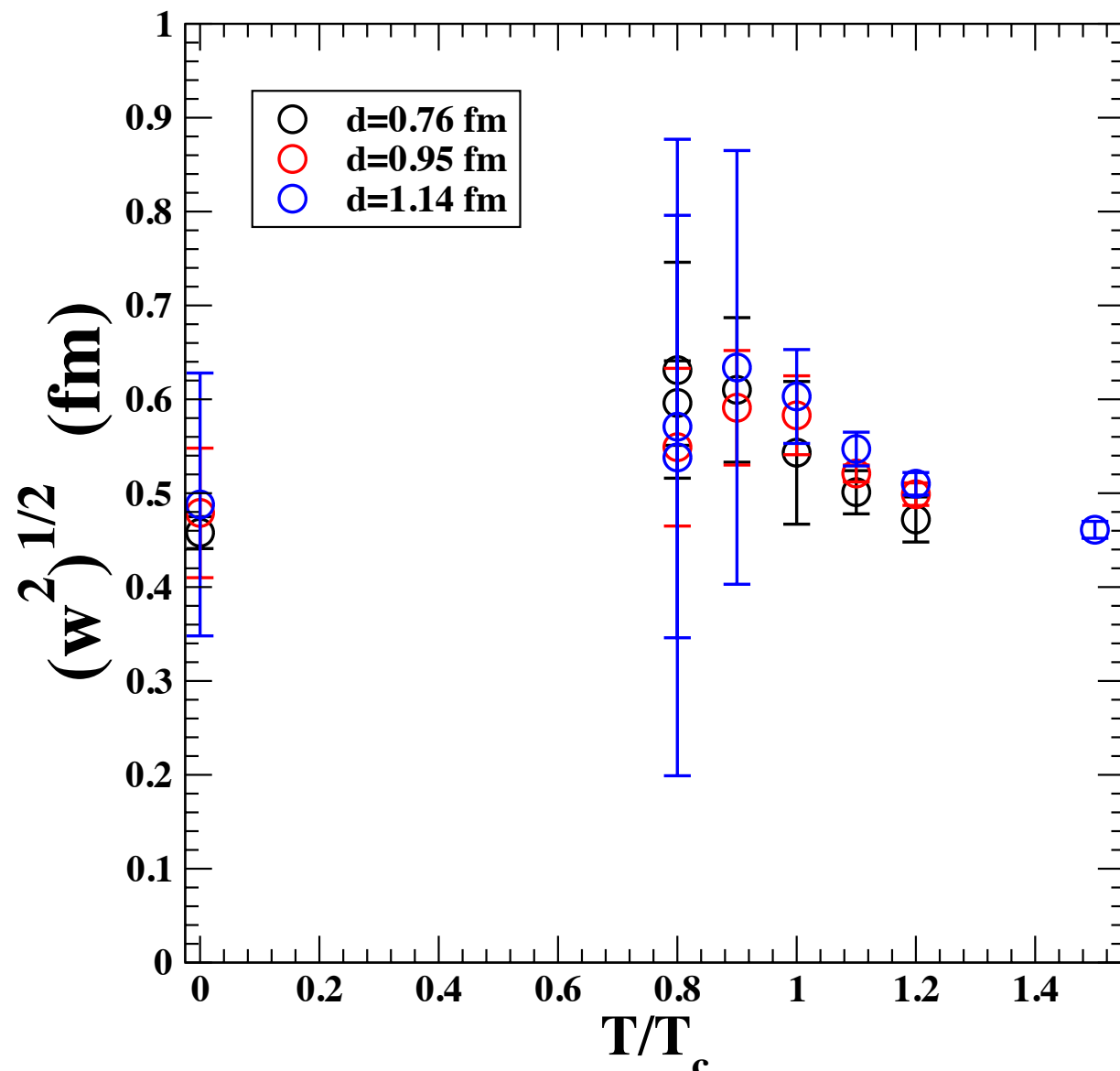


lambda almost constant across the phase transition

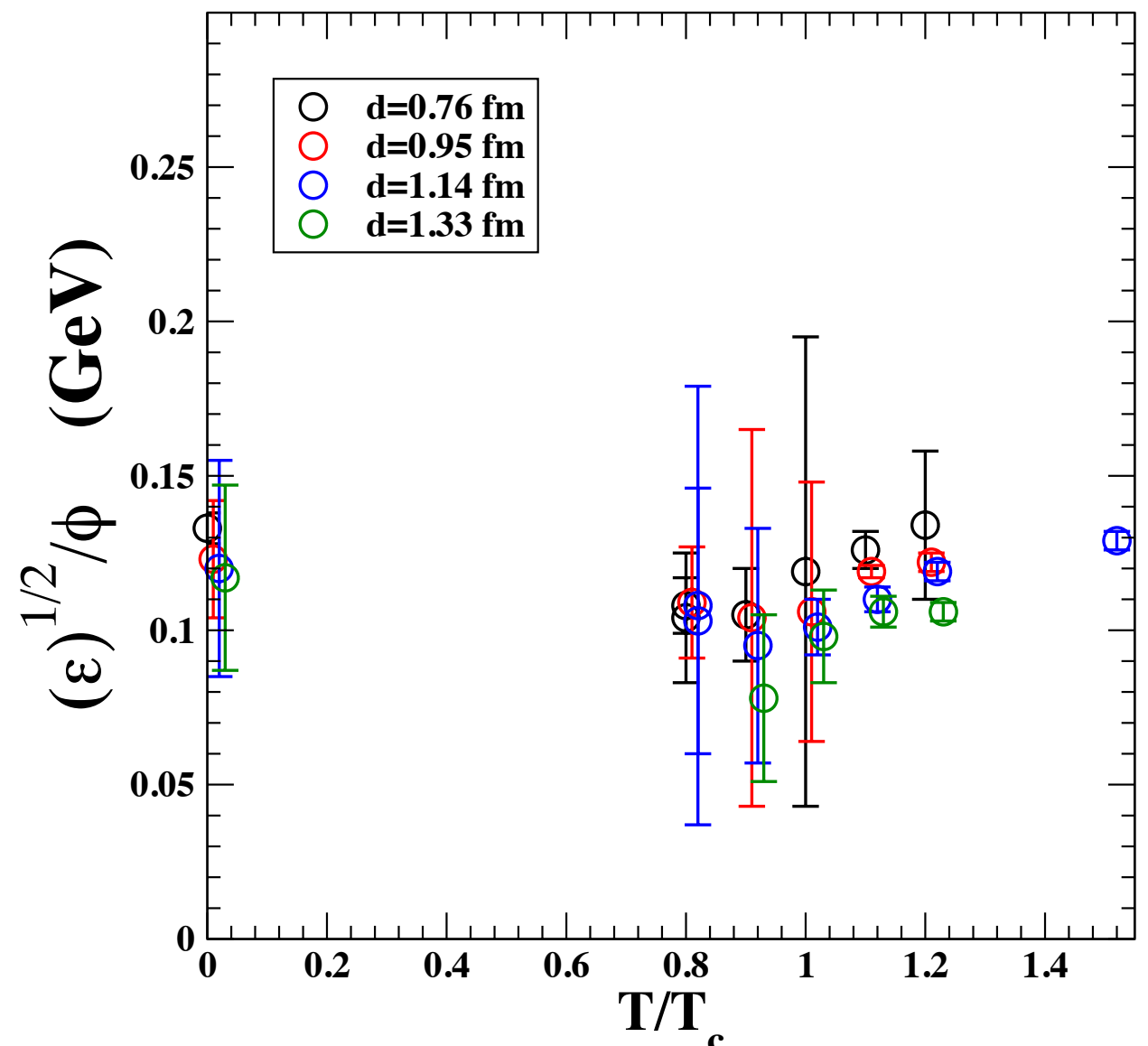
across deconfinement (cont'd)

$$\sqrt{w^2} = \sqrt{\frac{\int d^2x_t x_t^2 E_l(x_t)}{\int d^2x_t E_l(x_t)}}$$

$$\frac{\sqrt{\varepsilon}}{\phi} = \frac{\sqrt{\int d^2x_t \frac{E_l(x_t)^2}{2}}}{\phi}$$



almost constant across the phase transition



almost constant across the phase transition

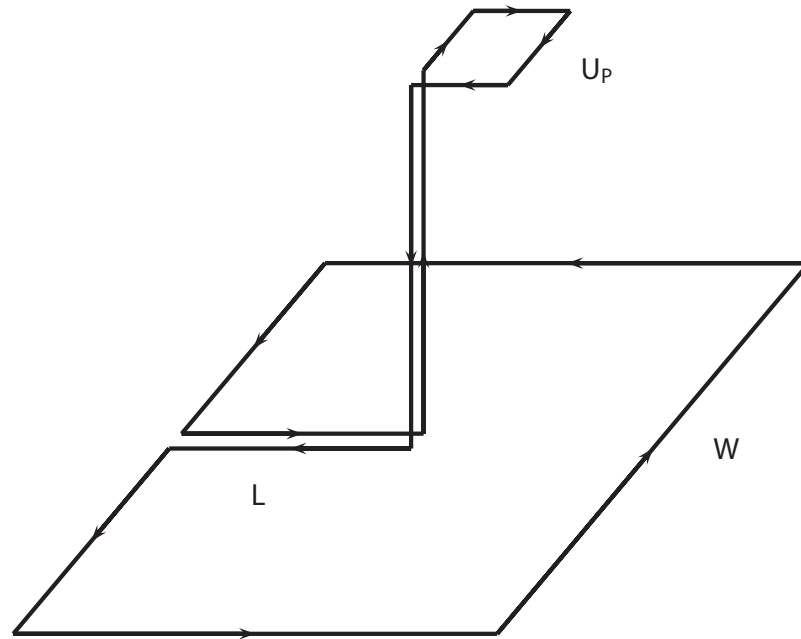
Summary & Outlook

- We have studied the flux tubes produced by a quark-antiquark pair in the case of SU(3) pure gauge theory across deconfinement phase transition.
- We have seen that the transverse behavior of the field inside the flux tube can be well described using a functional form derived from ordinary superconductivity (“Clem fit”).
- The flux tube shape seems to survive across deconfinement up to $T=1.5 T_c$, even though the strength of the field collapses across the phase transition. At the moment we are not able to exclude that what we are seeing in the deconfined region is due to a screened Coulomb potential.
- We want to check the stability of our results under changes of the smoothing procedure.
- We want to study the fate of the flux tubes at finite temperature in QCD with (2+1) flavours (possibly using HotQCD configurations)



BACKUP SLIDES

Field strength tensor



$$\rho_W^{\text{conn}} = \frac{\langle \text{tr} (W L U_P L^\dagger) \rangle}{\langle \text{tr}(W) \rangle} - \frac{1}{N} \frac{\langle \text{tr}(U_P) \text{tr}(W) \rangle}{\langle \text{tr}(W) \rangle}$$

field strength tensor

$$F_{\mu\nu}(x) = \sqrt{\frac{1}{g^2}} \rho_W^{\text{conn}}(x)$$

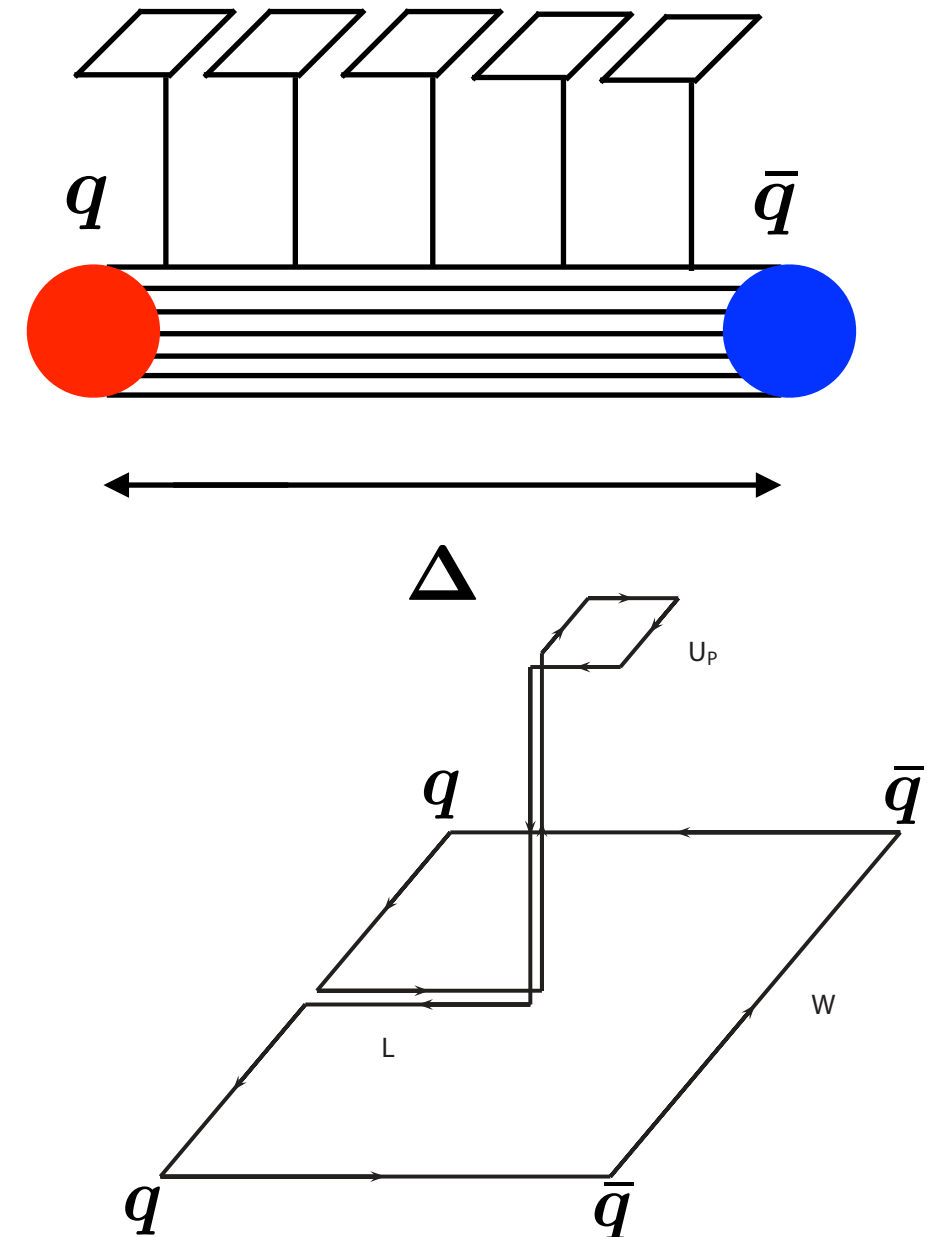
To specify better the color structure of the field $F_{\mu\nu}$, we note that the Wilson loop connected to the plaquette is the source of a color field which points, in average, onto an unknown direction n^a in color space, given by the loop itself (there is no preferred direction). What we measure is the average projection of the color field onto that direction. The color indices of the Schwinger lines are contracted with the loop, which is the source of the field, and realize the color parallel transport between the source loop and the plaquette position. For this reason, the $F_{\mu\nu}$ should be understood as:

$$F_{\mu\nu} \quad n^a F_{\mu\nu}^a$$

$$\rho_W^{\text{conn}} \xrightarrow{a \rightarrow 0} a^2 g \left(\left\langle n^a F_{\mu\nu}^a \right\rangle_{q\bar{q}} \right)$$

That this relation must hold and that the vector in color space n^a must be introduced follows from the linearity in the color field of the operator and from its gauge invariance.

Chromoelectric longitudinal field along the flux tube

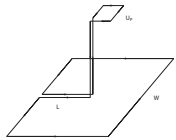


- ✓ Flux tube structure \longrightarrow tubular shape of the flux profile
- ✓ Chromoelectric longitudinal field constant along the flux tube (not too close to the static color sources)

Measuring the chromoelectric field on the lattice

$$F_{\mu\nu}(x) = \sqrt{\frac{1}{g^2}} \rho_W^{\text{conn}}(x)$$

Wilson loop

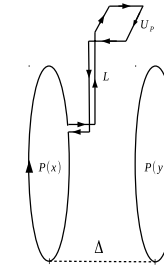


$$\rho_W^{\text{conn}} = \frac{\langle \text{tr}(W L U_P L^\dagger) \rangle}{\langle \text{tr}(W) \rangle} - \frac{1}{N} \frac{\langle \text{tr}(U_P) \text{tr}(W) \rangle}{\langle \text{tr}(W) \rangle}$$

$$\rho_W^{\text{conn}} \xrightarrow{a \rightarrow 0} a^2 g \left(\langle F_{\mu\nu} \rangle_{q\bar{q}} - \langle F_{\mu\nu} \rangle_0 \right)$$

$$\rho_W^{\text{conn}} \xrightarrow{a \rightarrow 0} a^2 g \left(\left\langle n^a F_{\mu\nu}^a \right\rangle_{q\bar{q}} \right)$$

Polyakov loop



$$\rho_P^{\text{conn}} = \frac{\langle \text{tr}(P(x) L U_P L^\dagger) \text{tr} P^\dagger(y) \rangle}{\langle \text{tr}(P(x)) \text{tr}(P^\dagger(y)) \rangle} - \frac{1}{N} \frac{\langle \text{tr}(P(x)) \text{tr}(P^\dagger(y)) \text{tr}(U_P) \rangle}{\langle \text{tr}(P(x)) \text{tr}(P^\dagger(y)) \rangle}$$

The operator is defined as trace of loops so it is gauge invariant. We have also seen that it changes sign by changing the orientation of the plaquette. So it is linear in the field. Therefore it cannot be that an average of the colour components of the field.

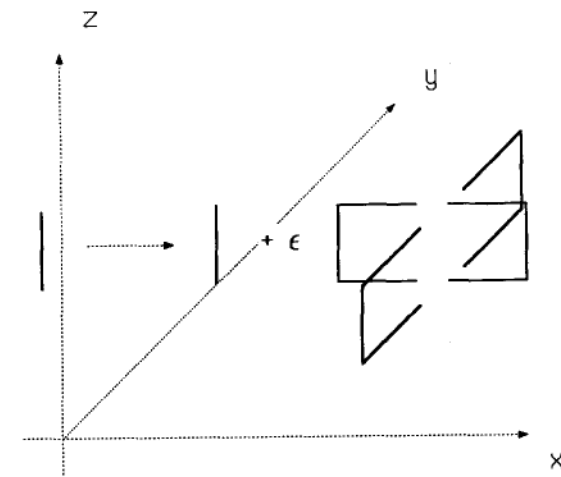
Renormalisation: the only thing that should be renormalised is the Schwinger line since it appears only at numerator. However since we observe scaling it seems that this renormalisation does not play an important role when we are close to the continuum limit.

smoothing of the gauge configurations

- remove the short distance fluctuations of the gauge field in order to improve the correlation signal
- local averages over short paths connecting the link's endpoints
- the long distance correlation signals should not be affected by smearing procedure (as long as the smearing is local enough)

APE smearing (on spatial links)

$$\bar{V}_{i,\mu;\nu} = Proj_{SU(3)} \left[(1-\alpha)U_{i,\mu} + \frac{\alpha}{4} \sum_{\pm\rho \neq \nu,\mu} U_{i,\rho;\nu\mu} U_{i+\hat{\rho},\mu;\rho\nu} U_{i+\hat{\mu},\rho;\nu\mu}^\dagger \right]$$



HYP smearing (on temporal links)

$$\text{1st step) } \bar{V}_{i,\mu;\nu\rho} = Proj_{SU(3)} \left[(1-\alpha_3)U_{i,\mu} + \frac{\alpha_3}{2} \sum_{\pm\eta \neq \rho,\nu,\mu} U_{i,\eta} U_{i+\hat{\eta},\mu} U_{i+\hat{\mu},\eta}^\dagger \right]$$

$$\text{2nd step) } \tilde{V}_{i,\mu;\nu} = Proj_{SU(3)} \left[(1-\alpha_2)U_{i,\mu} + \frac{\alpha_2}{4} \sum_{\pm\rho \neq \nu,\mu} \bar{V}_{i,\rho;\nu\mu} \bar{V}_{i+\hat{\rho},\mu;\rho\nu} \bar{V}_{i+\hat{\mu},\rho;\nu\mu}^\dagger \right]$$

$$\text{3rd step) } V_{i,\mu} = Proj_{SU(3)} \left[(1-\alpha_1)U_{i,\mu} + \frac{\alpha_1}{6} \sum_{\pm\nu \neq \mu} \tilde{V}_{i,\nu;\mu} \tilde{V}_{i+\hat{\nu},\mu;\nu} \tilde{V}_{i+\hat{\mu},\nu;\mu}^\dagger \right],$$

